Measurements of prompt fission γ-rays and neutrons with lanthanide halide scintillation detectors

A. Oberstedt

ERINDA workshop 2013
CERN, Switzerland

October 1 – 3, 2013

Outline

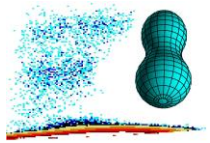

- Introduction
- Experiments: ^{252}Cf(sf), ^{235}U(n_{th}, f) and ^{241}Pu(n_{th}, f)
  - technique(s)
  - instrumentation
  - electronics
- Data treatment
- Results
  - prompt fission neutron spectra (PFNS)
  - prompt fission γ-ray spectra (PFGS)
- Summary
- Outlook

Introduction

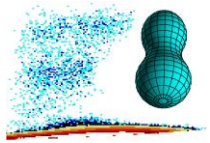

The fission process and nuclear power

Energy dissipation

Introduction

The fission process and nuclear power

prompt neutrons (< 10^{-18} s)

prompt γ-rays (10^{-16} s)

fission fragments (10^{-21} s)

ternary α, t, d, ^{10}Be…

kinetic energy prompt γ-rays	heat
prompt neutrons (delayed neutrons)	chain reaction
ternary α, t, d	gas production in the fuel (waste)
fission fragments	decay heat, toxicity (waste)

Introduction
Energy dissipation

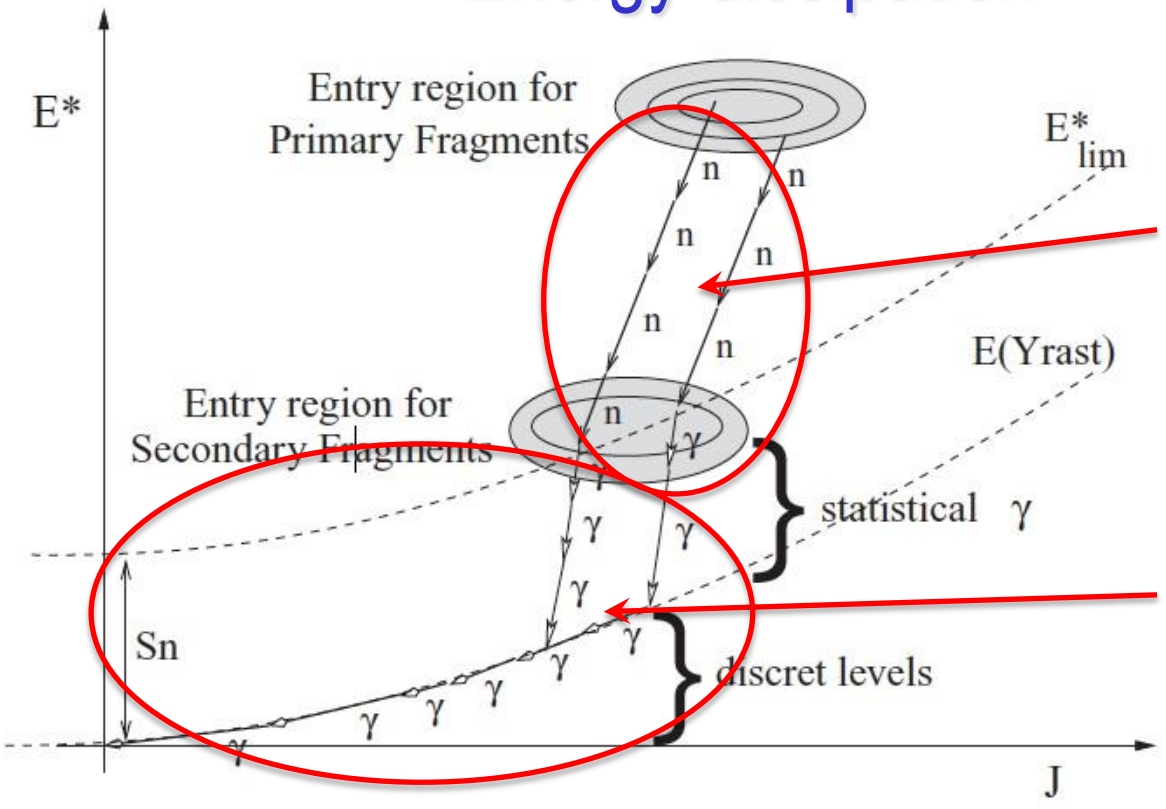

prompt neutrons

prompt γ-rays

O. Litaize and O. Serot,
PRC 82, (2010)

FIG. 2. Schematic representation of the evaporation of the fission fragments in the (E^*, J) plan. Primary fragments dissipate excitation energy E^* through neutron emission until $E^* < S_n + E^{rot}$ while secondary fragments dissipate energy through γ rays.

Experiments

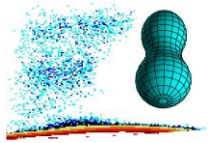

Technique(s)

Instrumentation

Electronics

Experiments
Technique(s)

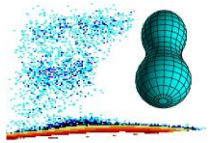

- Coincidence measurements of neutrons and γ-rays with fission fragments
- Time-of-flight (TOF) measurements
- Discrimination of neutrons and γ-rays by their respective time-of-flight (TOF)
- Applied to $^{252}Cf(sf)$ at IRMM in Geel as well as $^{235}U(n_{th}, f)$ and $^{241}Pu(n_{th}, f)$ at IKI in Budapest

Experiments
Instrumentation

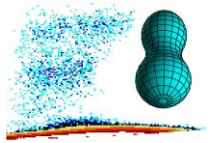

- Measurement of fission fragments with
  - VERDI / polycrystalline chemical vapour deposited (pCVD) diamond detectors [1]
  - (Frisch-grid) ionization chamber

- Measurement of neutrons and γ-rays with
  - lanthanide halide scintillation detectors ($LaCl_3$:Ce [2], $LaBr_3$:Ce [3,4], $CeBr_3$ [5,6])

1 S. Oberstedt et al., NIM A714 (2013)

2 A. Oberstedt et al., NIM A668 (2012)
3 A. Oberstedt et al., NIM A708 (2013)
4 R. Billnert et al., PRC 87 (2013)
5 R. Billnert et al., NIMA A647 (2011)
6 G. Lutter et al., NIM A703 (2013)

Experiments
Electronics

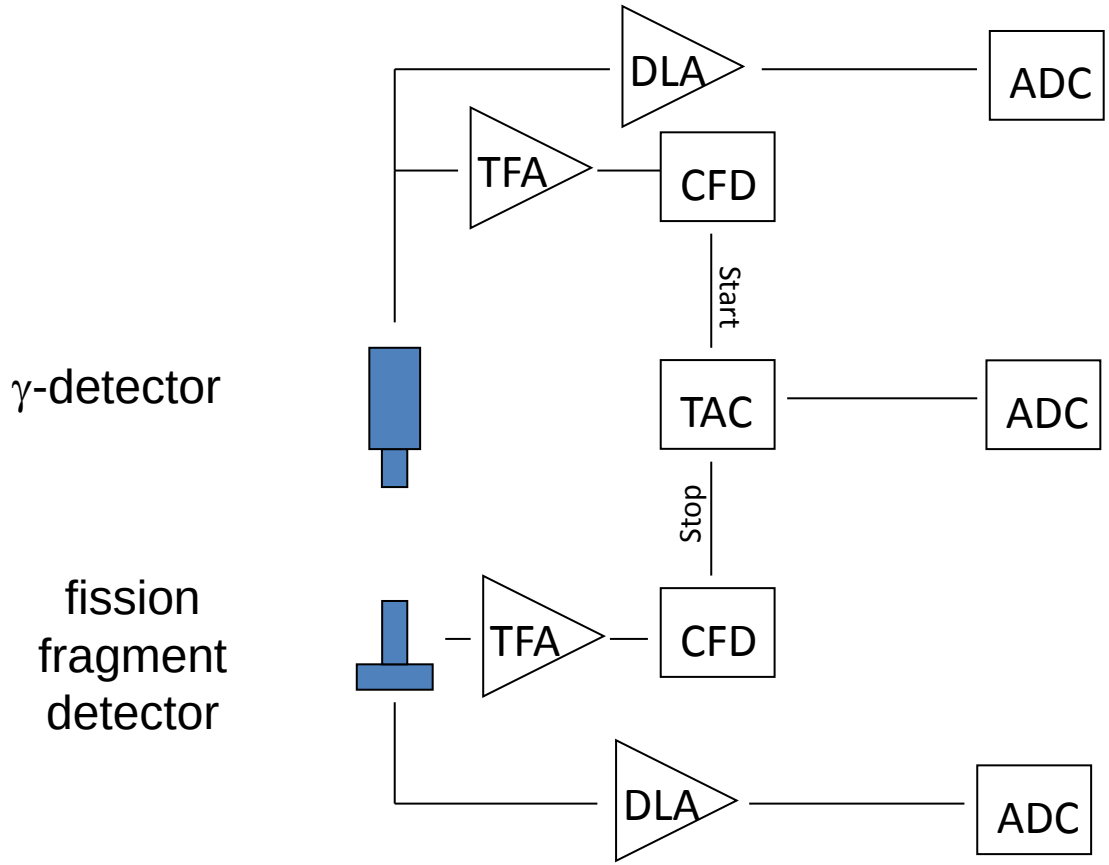

For each γ-detector: PH and TOF stored.

Data treatment

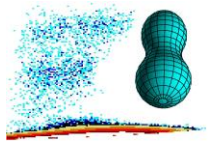

TOF vs. E

Particle identification

n/γ discrimination

γ response function

Data treatment

2-dim presentation: tof versus E

^{252}Cf(sf) and $LaBr_3$:Ce (2” x 2”)

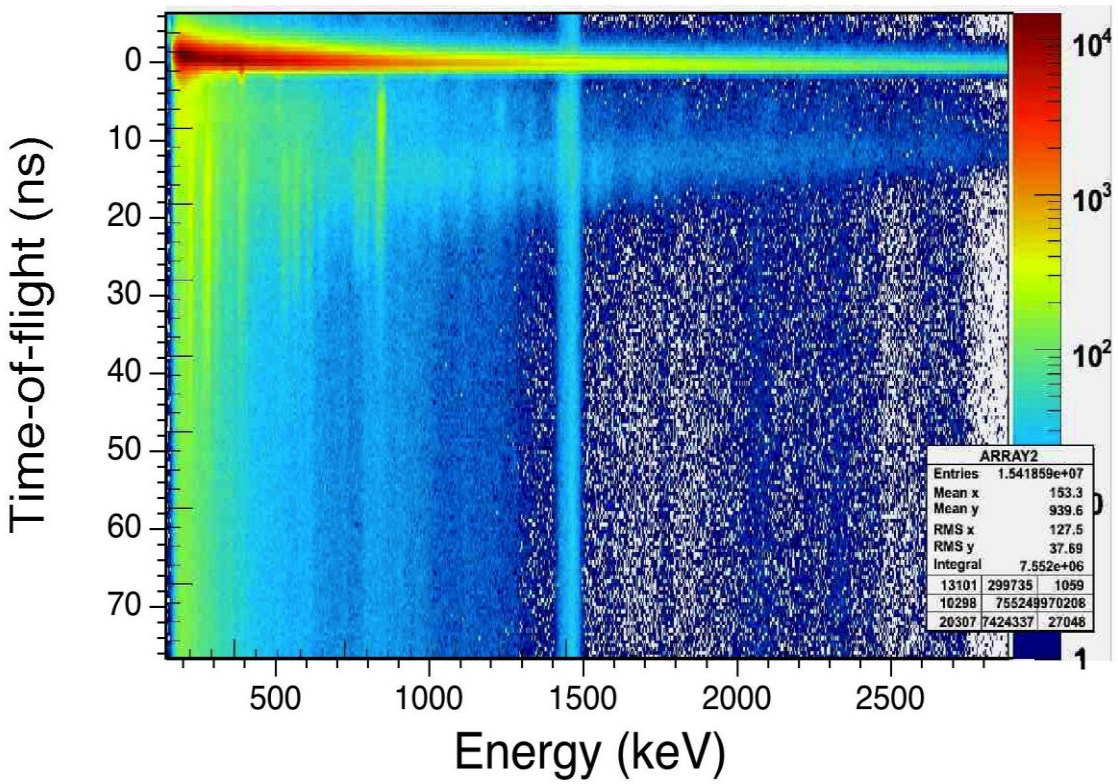

Photons in coincidence with fission fragments

Data treatment
Particle identification

^{252}Cf(sf) and $LaBr_3$:Ce (2” x 2”)

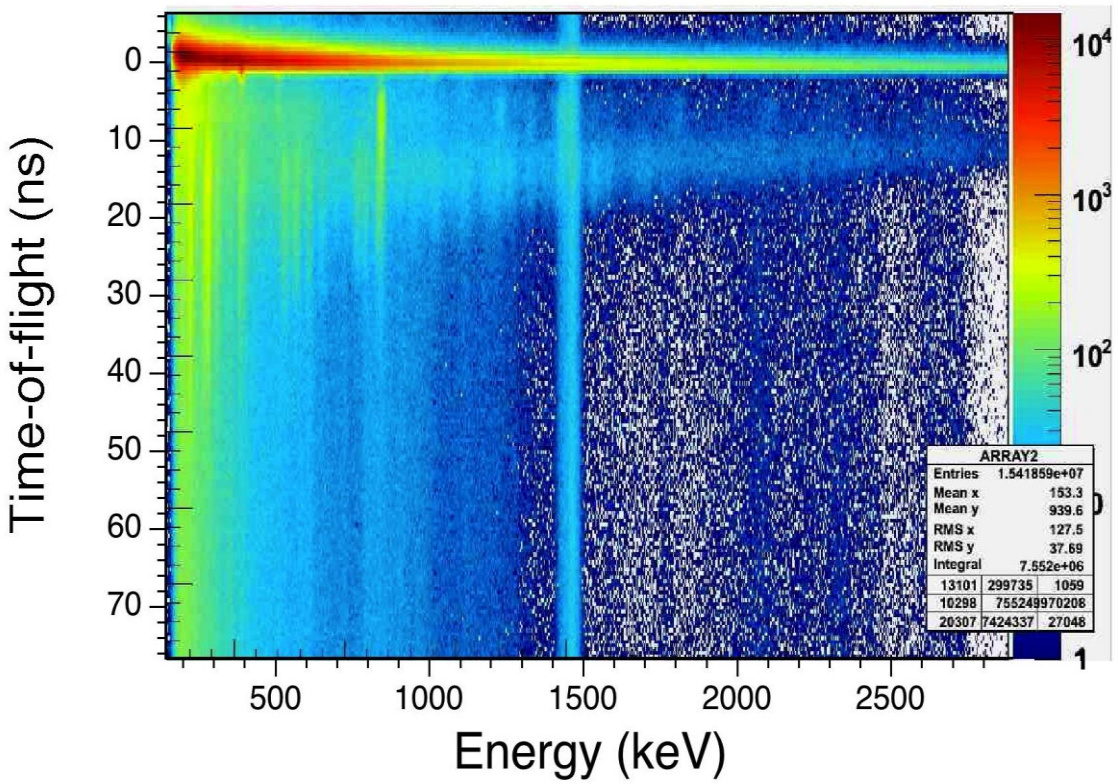

Photons in coincidence with fission fragments

Data treatment
Particle identification

^{252}Cf(sf) and $LaBr_3$:Ce (2” x 2”)

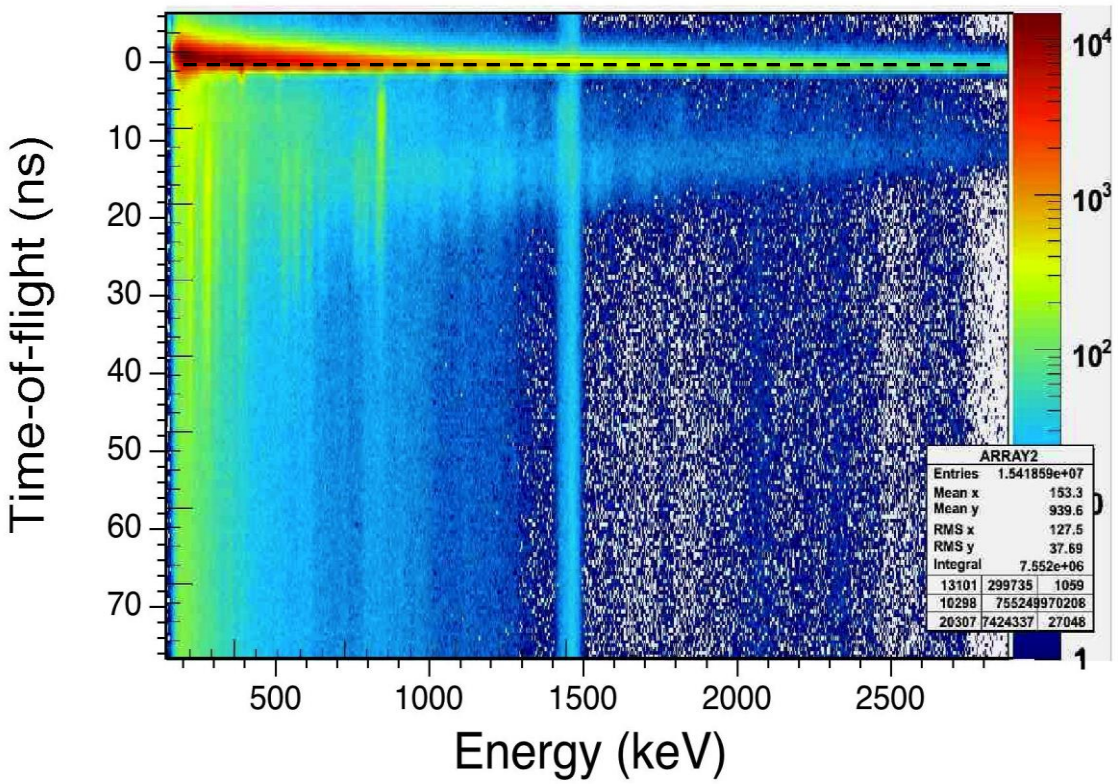

Prompt fission γ-rays

Photons in coincidence with fission fragments

Data treatment
Particle identification

^{252}Cf(sf) and $LaBr_3$:Ce (2” x 2”)

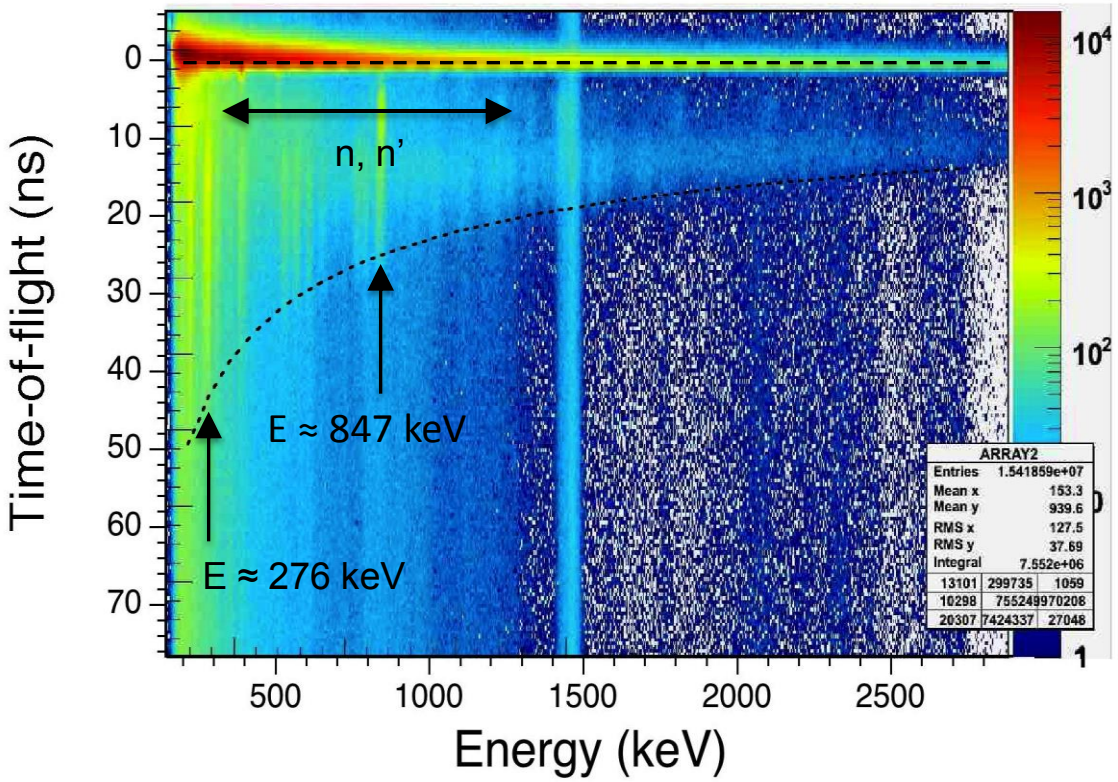

Prompt fission γ-rays

γ-decay after inelastic neutron scattering

Photons in coincidence with fission fragments

Data treatment
Particle identification

^{252}Cf(sf) and $LaBr_3$:Ce (2” x 2”)

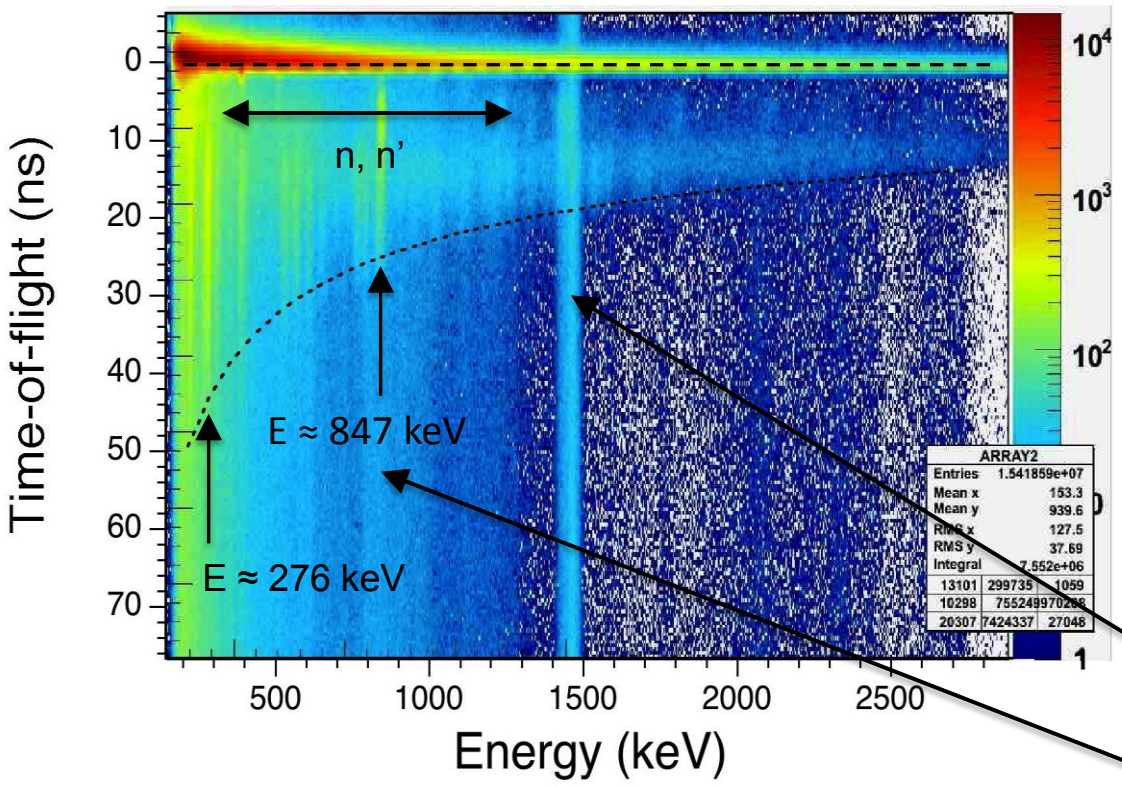

Prompt fission γ-rays

γ-decay after inelastic neutron scattering

Intrinsic and external background

Photons in coincidence with fission fragments

Data treatment

Neutron identification

^{252}Cf(sf) and $LaBr_3$:Ce (2” x 2”)

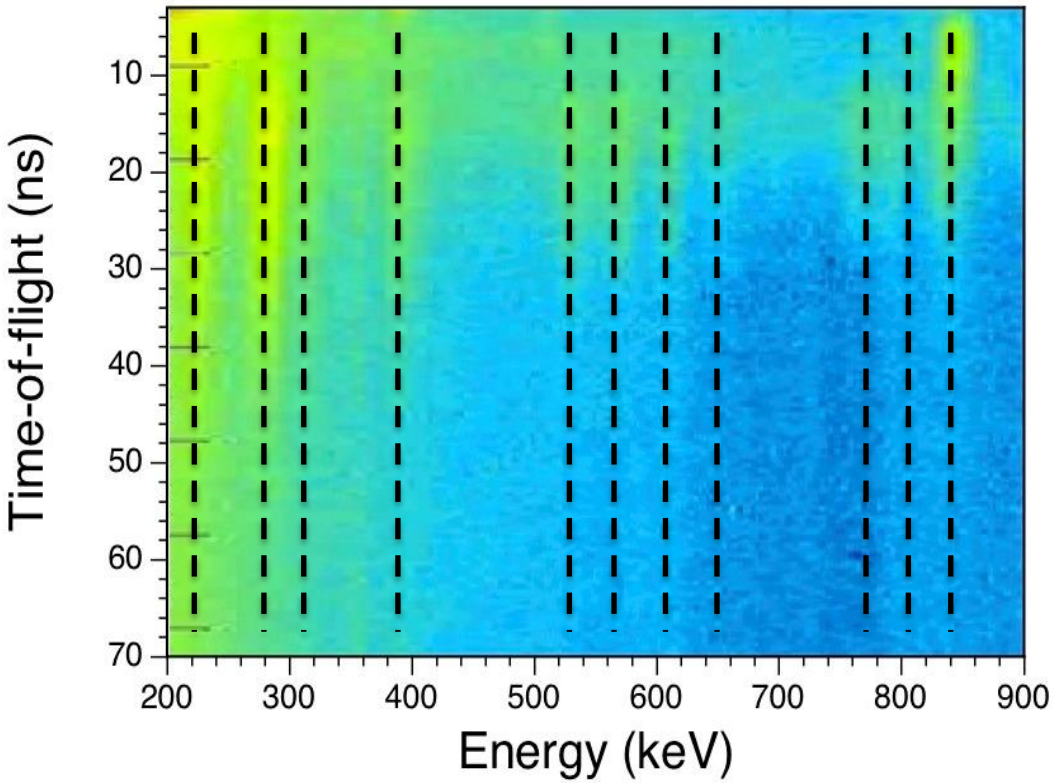

Focus on events from inelastic neutron scattering, exhibits discrete γ-lines → projection …

Data treatment

Energy spectrum

^{252}Cf(sf) and $LaBr_3$:Ce (2” x 2”)

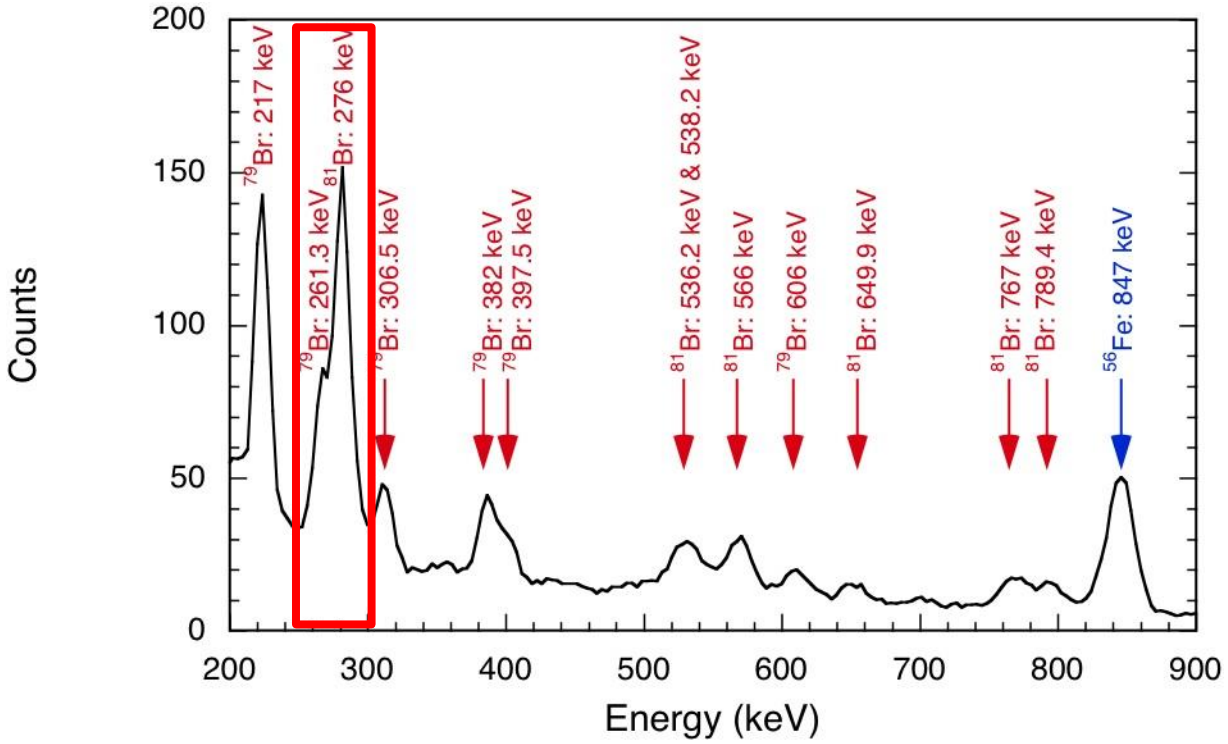

… identified as γ-decays of ^{79,81}Br* and ^{56}Fe*!

→ Examine tof distribution for E = (244 - 297) keV

Data treatment

Time-of-flight spectrum

^{252}Cf(sf) and $LaBr_3$:Ce (2” x 2”)

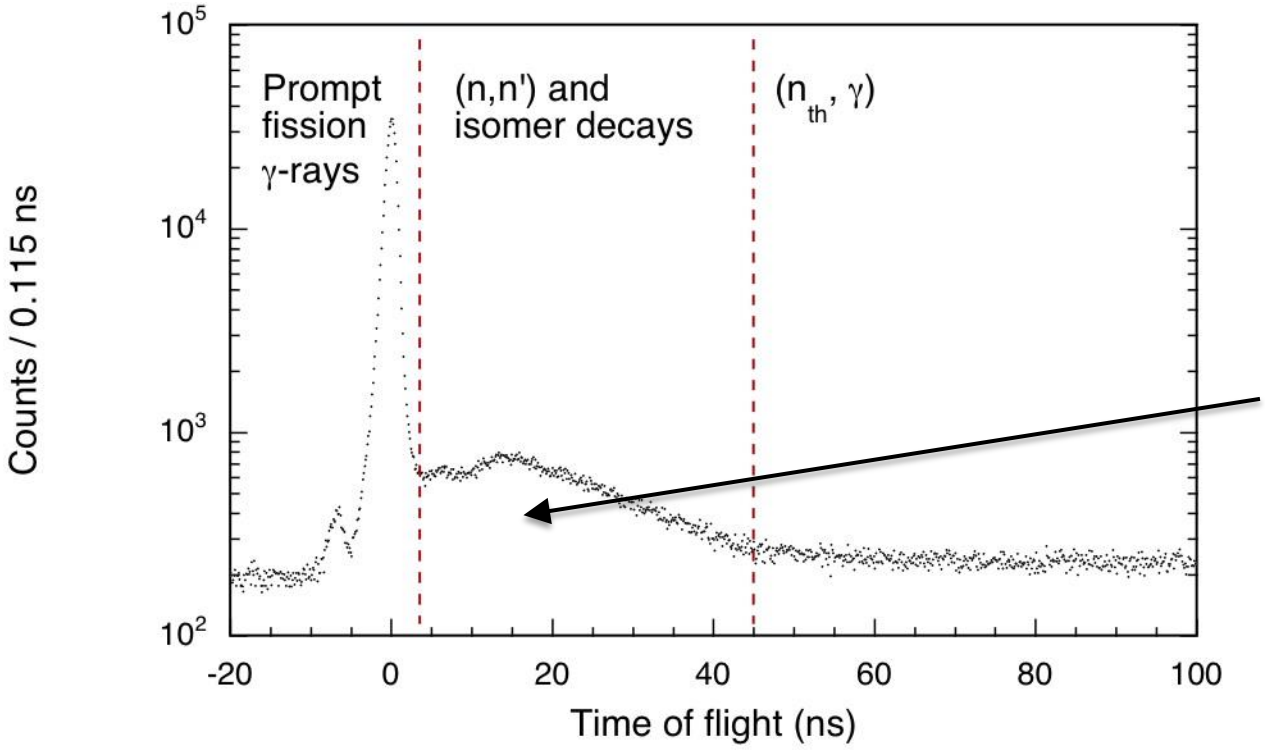

Region of interest

E = (244 - 297) keV

Data treatment

Time-of-flight spectrum

^{252}Cf(sf) and $LaBr_3$:Ce (2” x 2”)

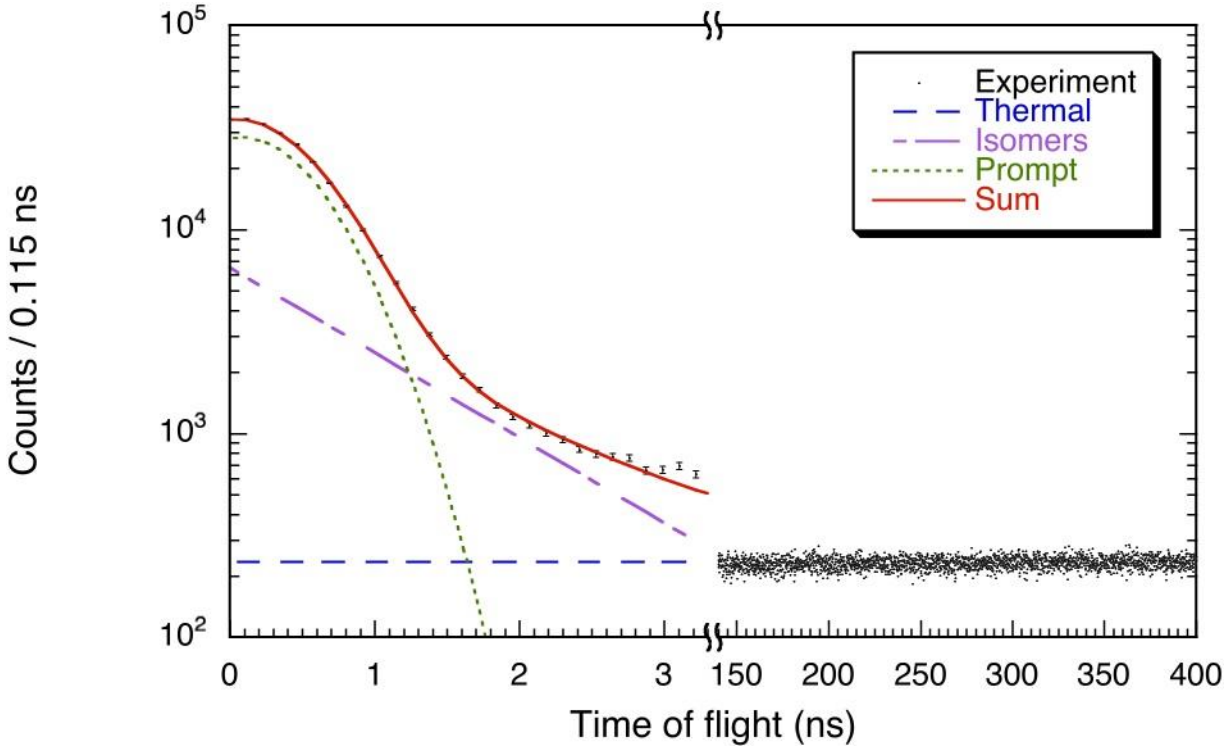

Background assessment …

Data treatment

Time-of-flight spectrum

^{252}Cf(sf) and $LaBr_3$:Ce (2” x 2”)

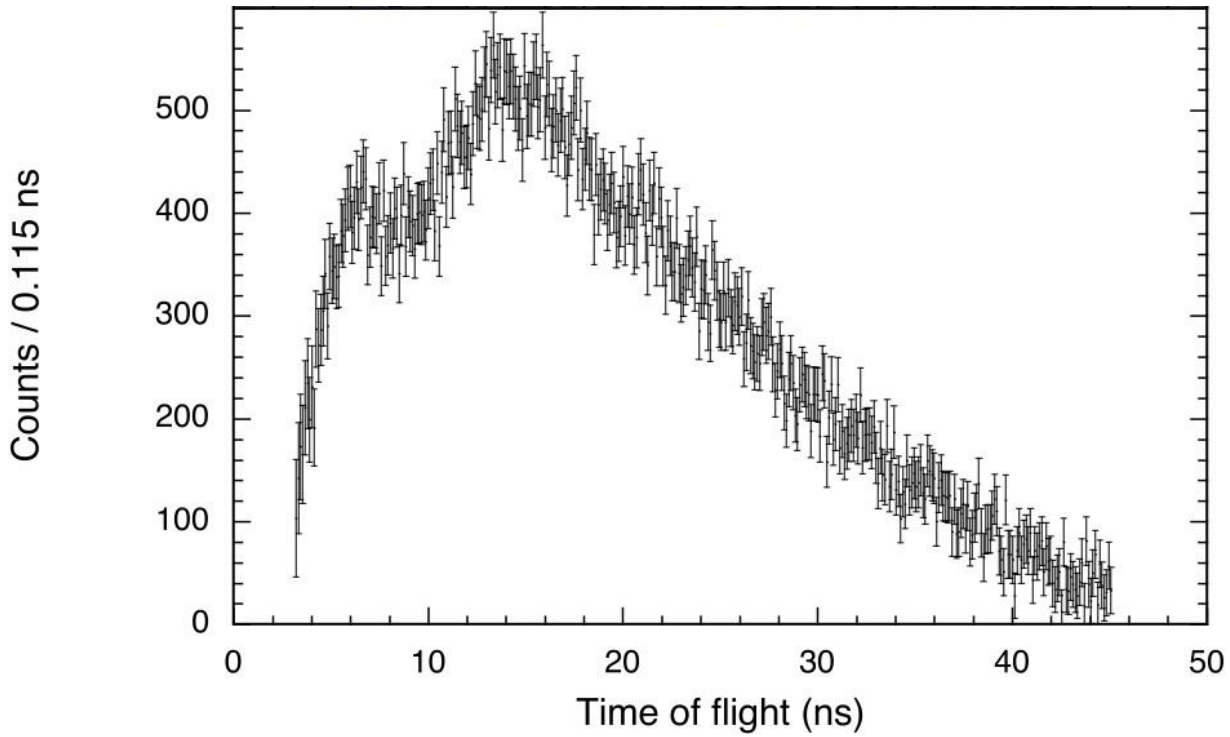

… and background subtraction!

Data treatment
Neutron efficiency

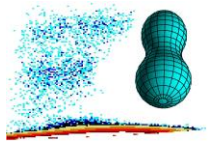

Determination of

$$\varepsilon_n = R_{\mathrm{det}} / R_{hit}$$

with R_{det} = detection rate from time-of-flight spectrum (measured)

and R_{hit} = hit rate from activity (known), geometry (known) and neutron spectrum (known: Mannhart evaluation).

Finally: conversion from time-of-flight to energy.

Data treatment

Prompt fission γ-ray identification

^{252}Cf(sf) and $LaBr_3$:Ce (2” x 2”)

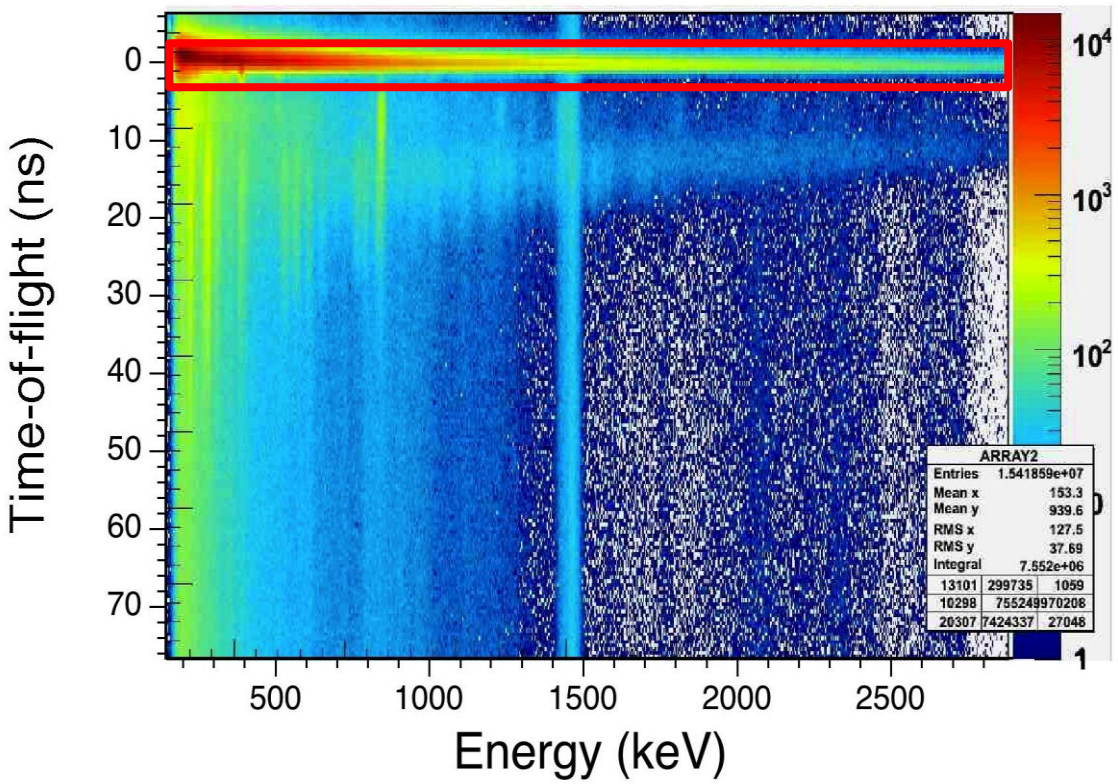

Photons in coincidence with fission fragments

Data treatment

Measured γ-ray spectra

^{252}Cf(sf) and $LaBr_3$:Ce (2” x 2”)

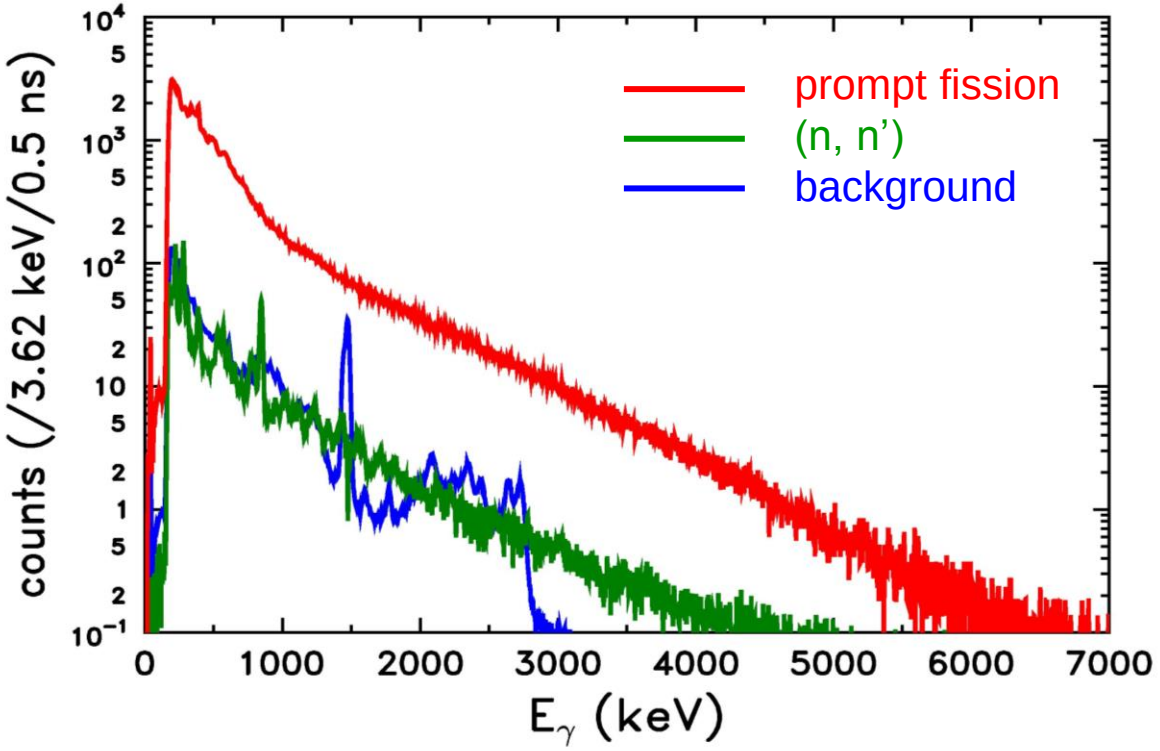

Background assessment and subtraction …

Data treatment

Measured prompt fission γ-ray spectrum

^{252}Cf(sf) and $LaBr_3$:Ce (2” x 2”)

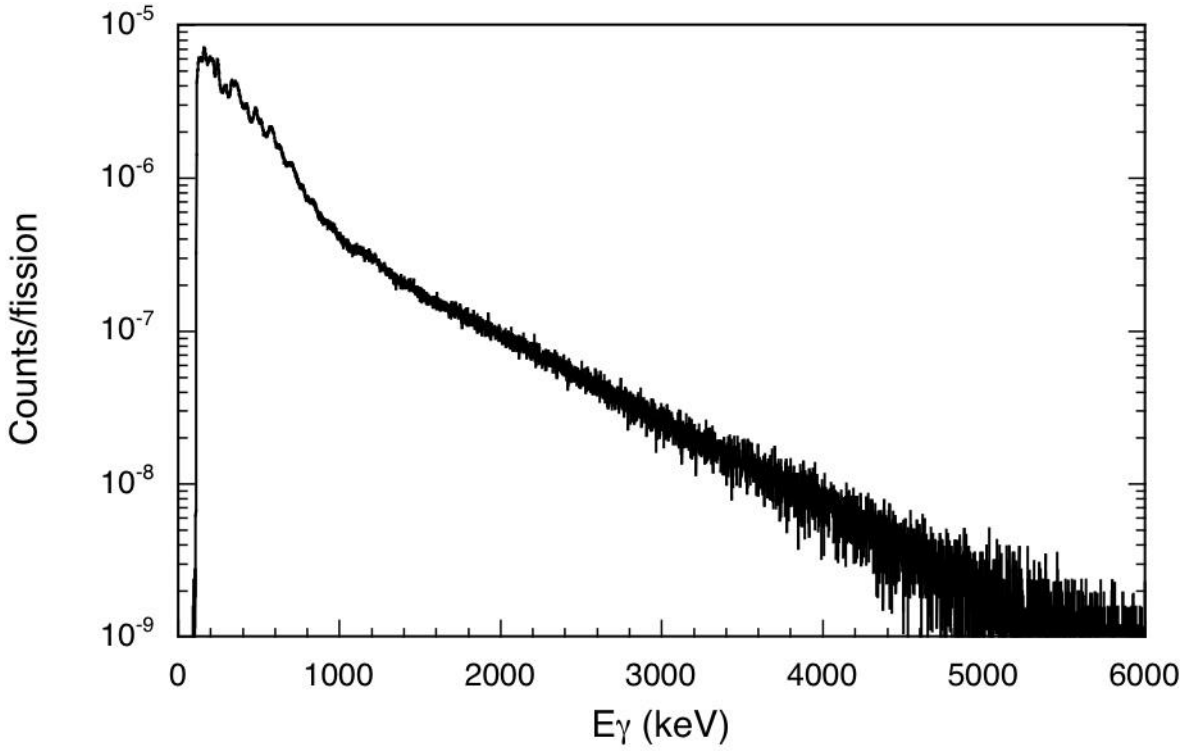

Unfolding response function …

Data treatment
Response function with PENELOPE

$LaBr_3$:Ce (2” x 2”)

R. Billnert, Annual report 2012 (IRMM)

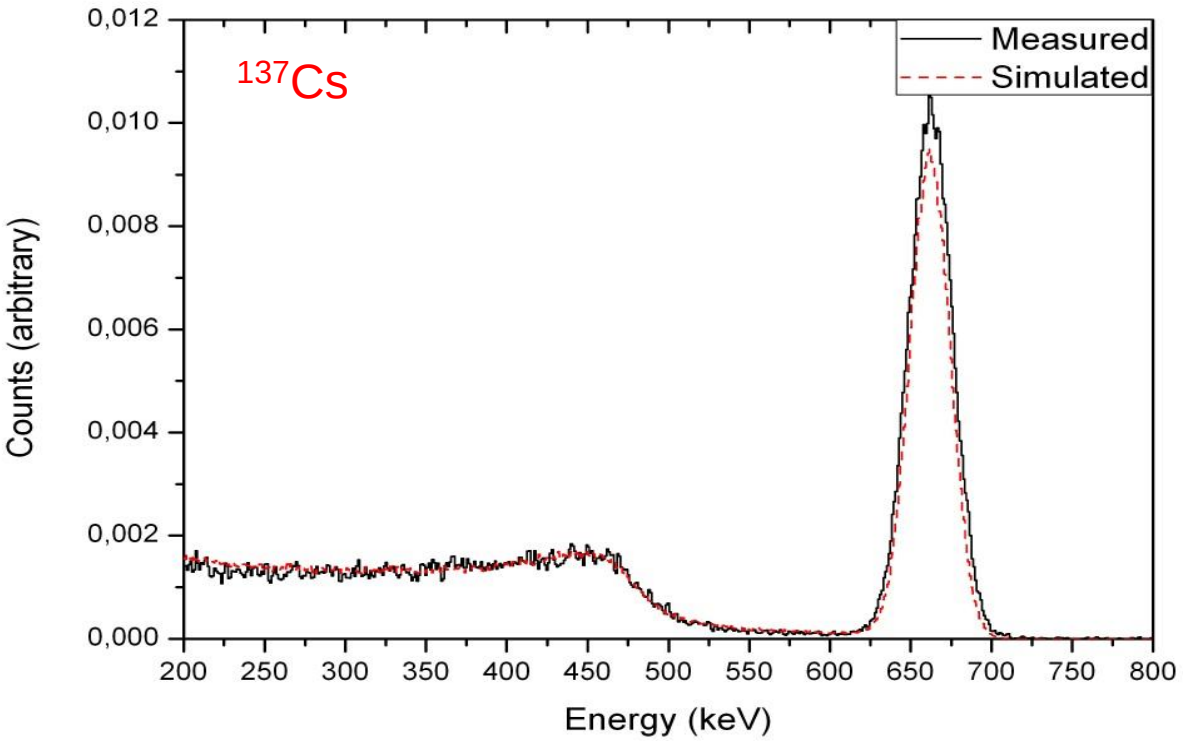

Good agreement!

Data treatment

Unfolding response function (illustration)

^{252}Cf(sf) and $LaBr_3$:Ce (2” x 2”)

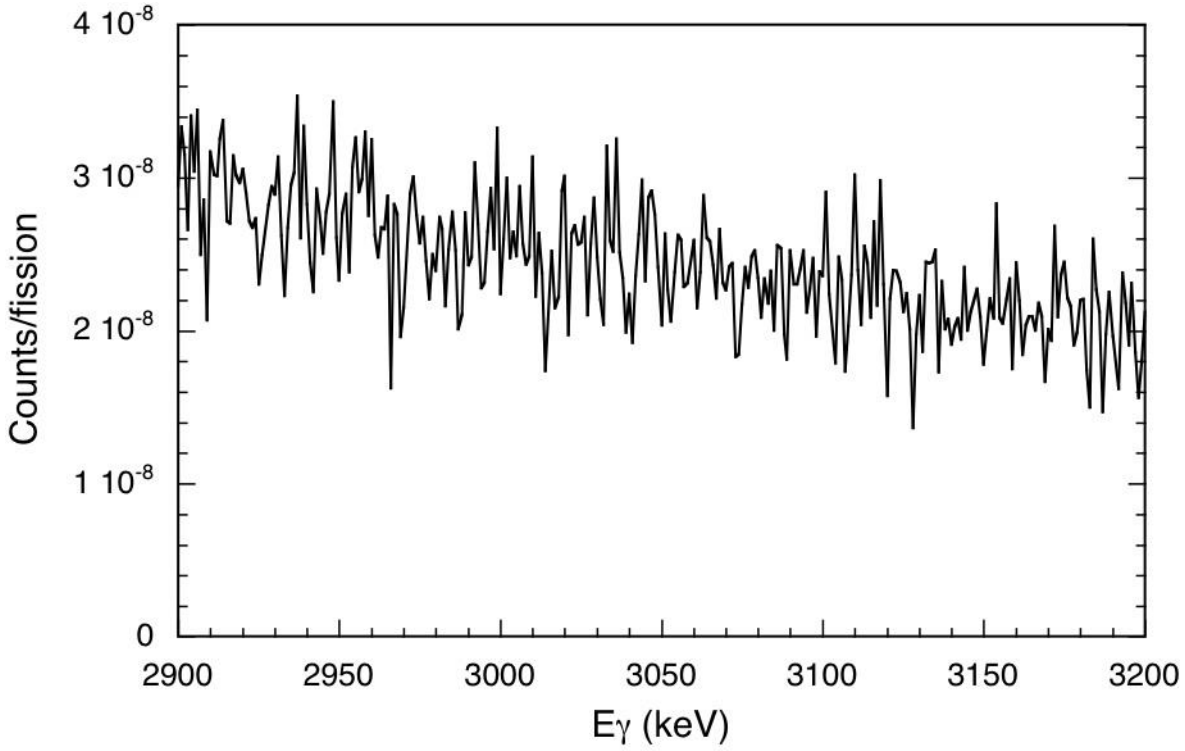

Measured prompt fission γ-ray energy spectrum

→ e.g. zooming into region around 3 MeV

Data treatment

Unfolding response function (illustration)

$LaBr_3$:Ce (2” x 2”)

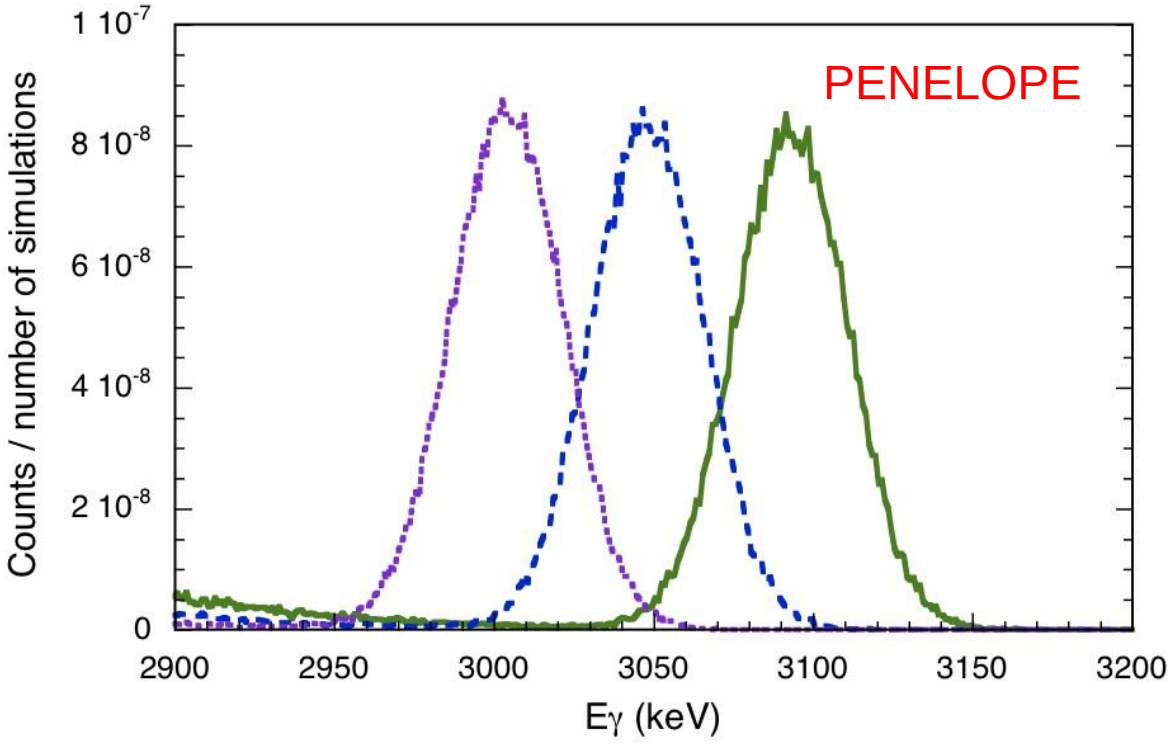

Simulating response function for mono-energetic γ-rays, distance: FWHM from energy resolution measurements

Data treatment

Unfolding response function (illustration)

^{252}Cf(sf) and $LaBr_3$:Ce (2” x 2”)

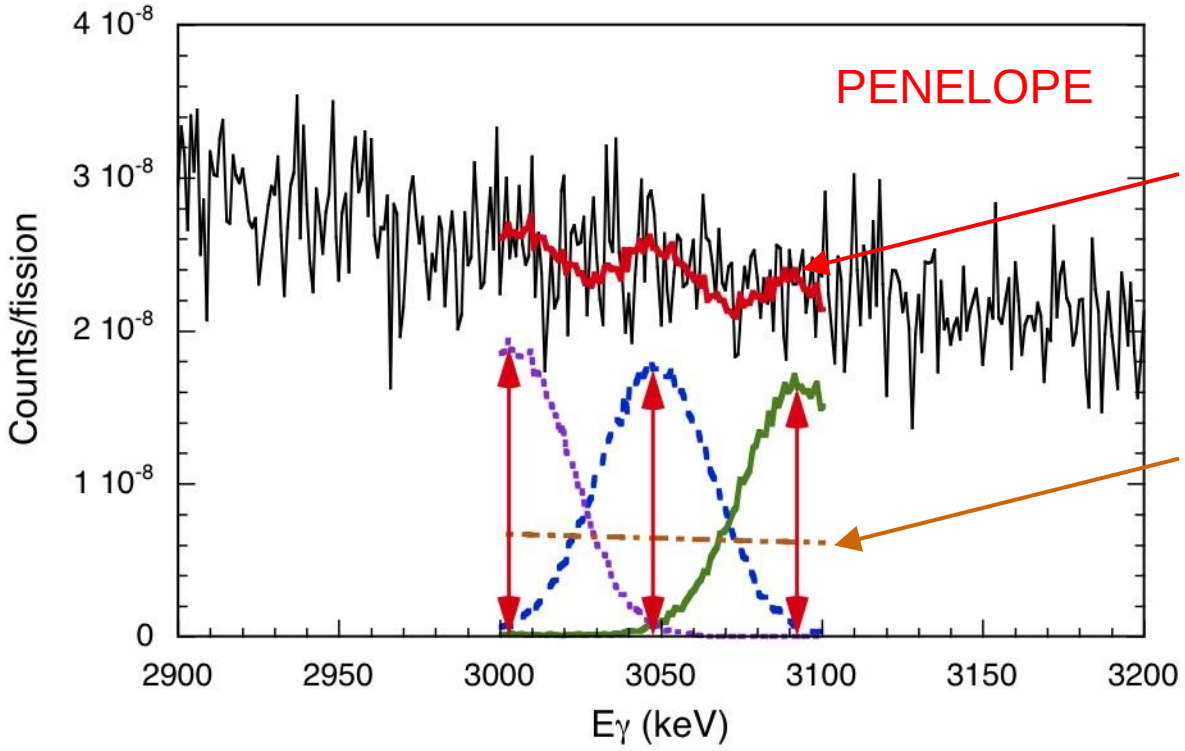

Adjusting simulated mono-energetic spectra to measured γ-ray spectrum and determining the scaling factors …

Data treatment

Unfolding response function (illustration)

^{252}Cf(sf) and $LaBr_3$:Ce (2” x 2”)

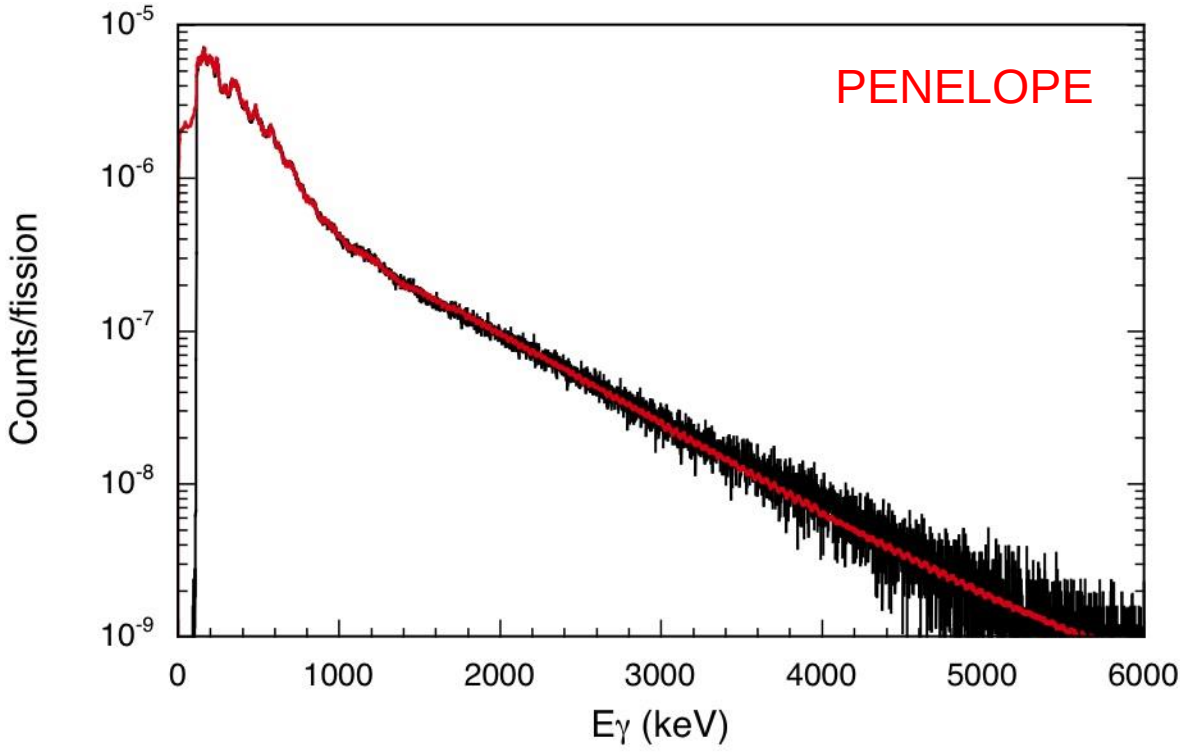

Adjusting simulated mono-energetic spectra to measured γ-ray spectrum and determining the scaling factors over entire energy region …

Data treatment

Unfolding response function (illustration)

^{252}Cf(sf) and $LaBr_3$:Ce (2” x 2”)

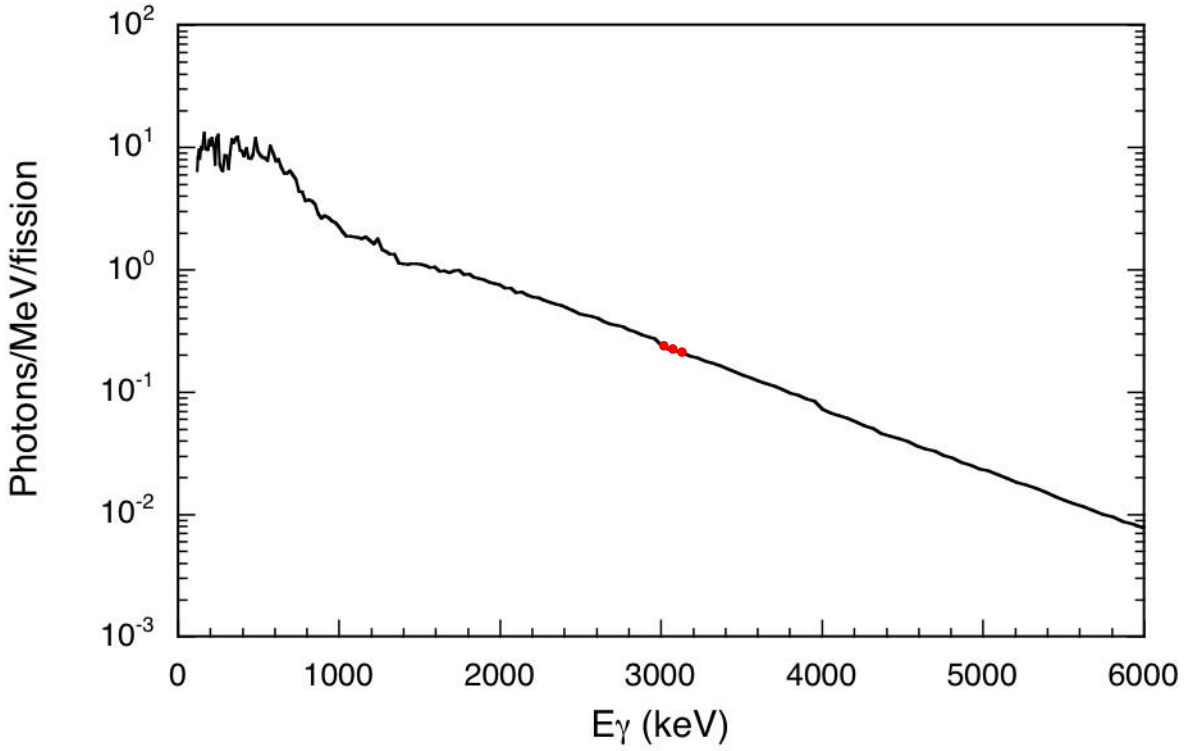

… and properly normalized scaling factors

→ emission spectrum!

Results

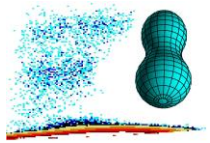

Prompt fission neutrons

- neutron efficiency of $LaBr_3$:Ce detector
- prompt fission neutron spectrum (PFNS) from $^{235}U(n_{th}, f)$

Prompt fission γ-rays from $^{252}Cf(sf)$, $^{235}U(n_{th}, f)$ and $^{241}U(n_{th}, f)$

- prompt fission neutron spectrum (PFGS)
- average multiplicity
- mean energy per photon
- total photon energy

Results

Neutron efficiency

^{252}Cf(sf) and $LaBr_3$:Ce (2” x 2”)

A. Oberstedt et al., NIM A708 (2013)

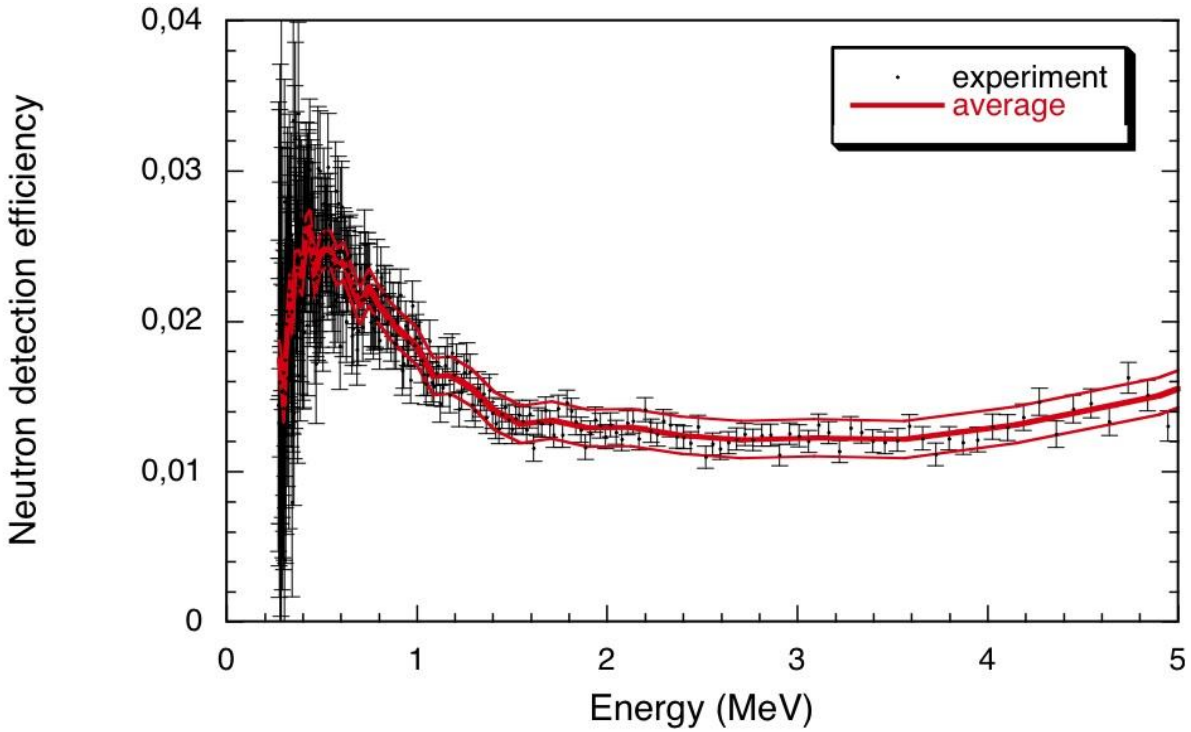

To be applied on data from $^{235}U(n_{th}, f)$.

Results

2-dim presentation: tof versus E

$^{235}U(n_{th}, f)$ and $LaBr_3$:Ce (2” x 2”)

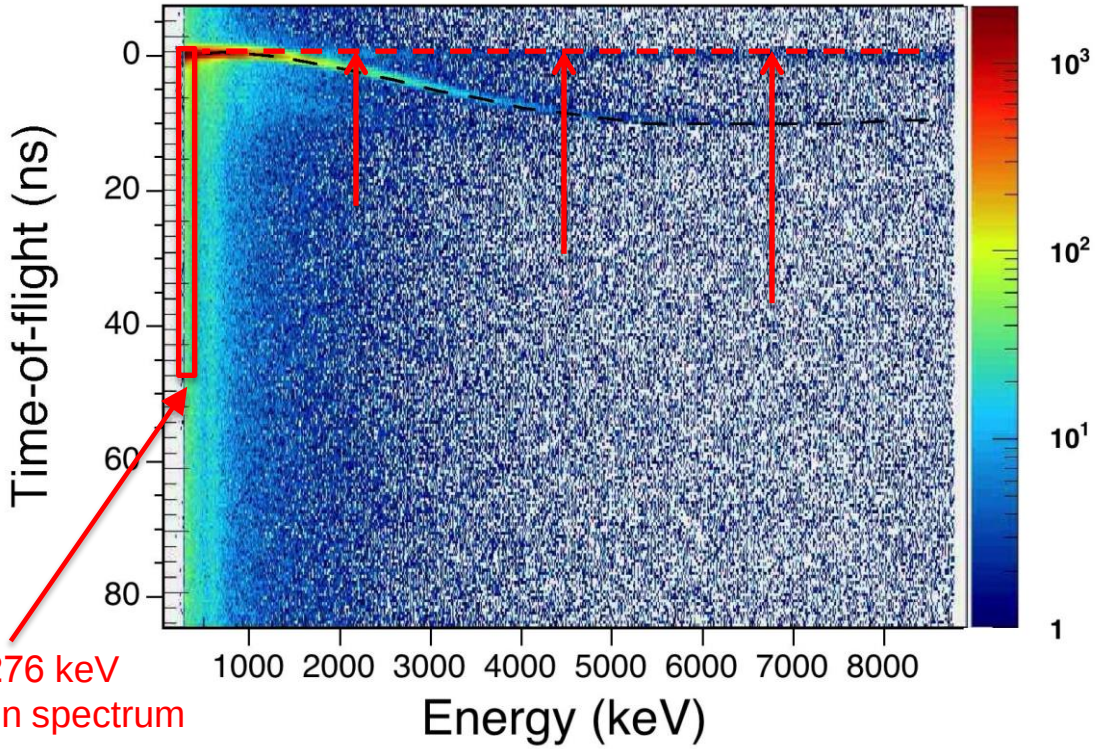

However, several problems were encountered with $LaBr_3$:Ce detector:

- PH dependence of TAC signal (corrected for)
- not properly working dynode output (PH)
- loss of events

Results

$^{235}U(n_{th}, f)$ PFNS

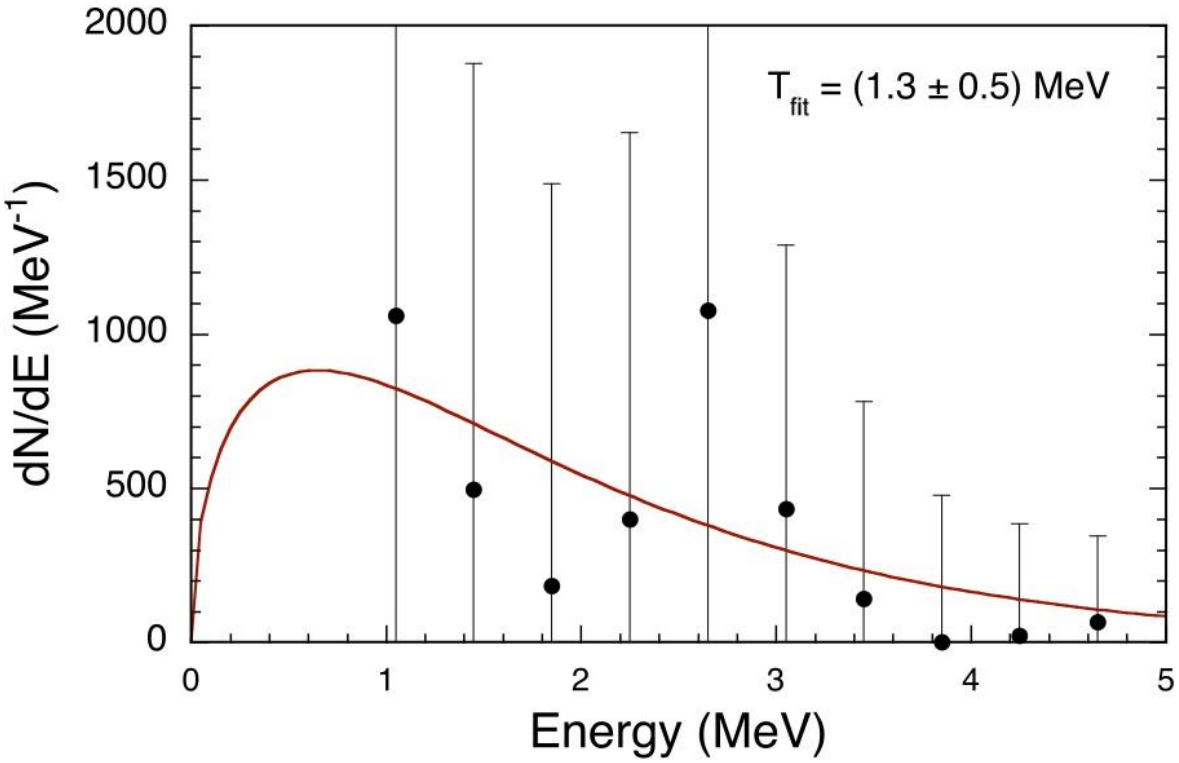

Boltzmann distribution fitted to data (cf. literature: T = 1.29 MeV). However, due to problems with low energy background assessment and poor statistics: only illustration!

Results
PFGS

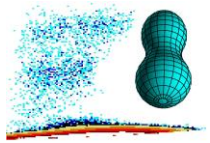

^{252}Cf(sf)

Results
^{252}Cf(sf) PFGS

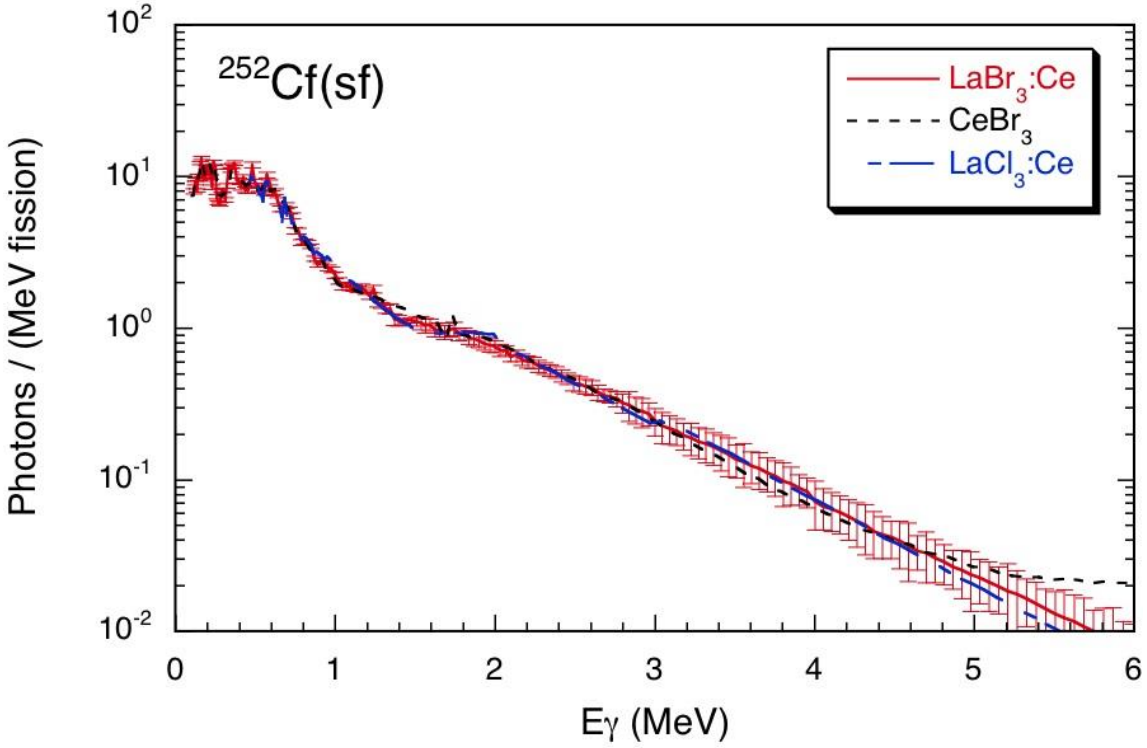

Excellent agreement between spectra taken with three different detectors, …

Results
^{252}Cf(sf) PFGS

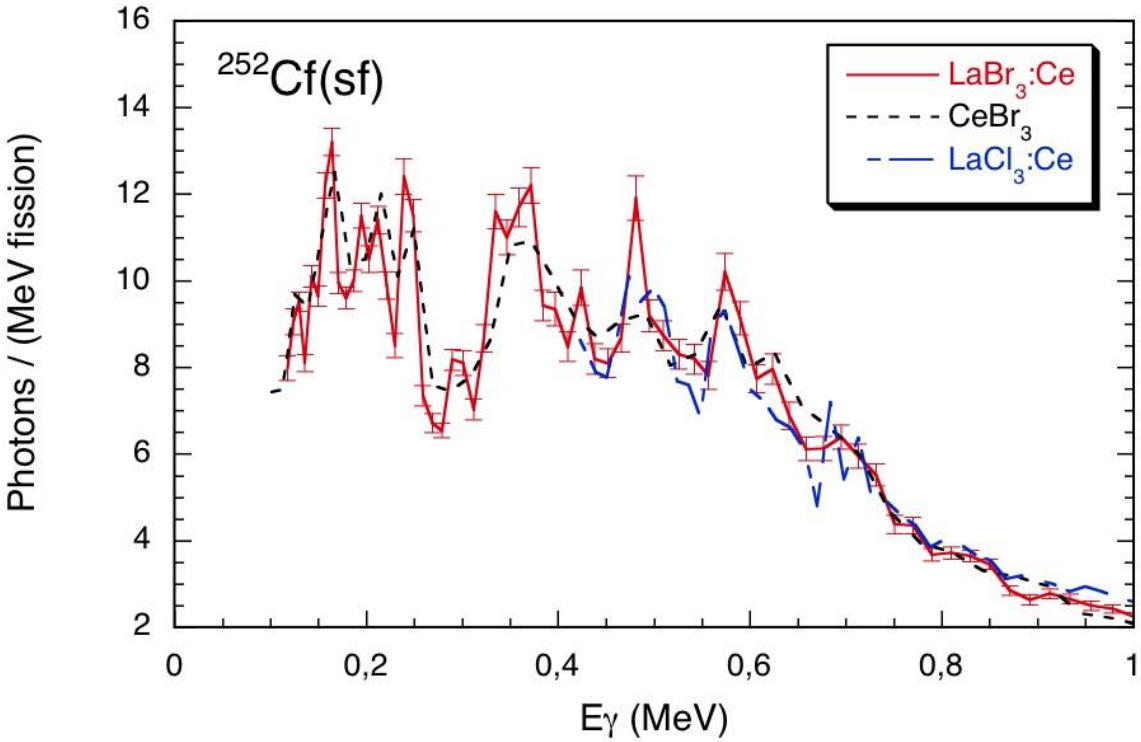

… even the discrete structure below 1 MeV is well reproduced!

Results
^{252}Cf(sf) PFGS

R. Billnert et al., PRC 87 (2013)

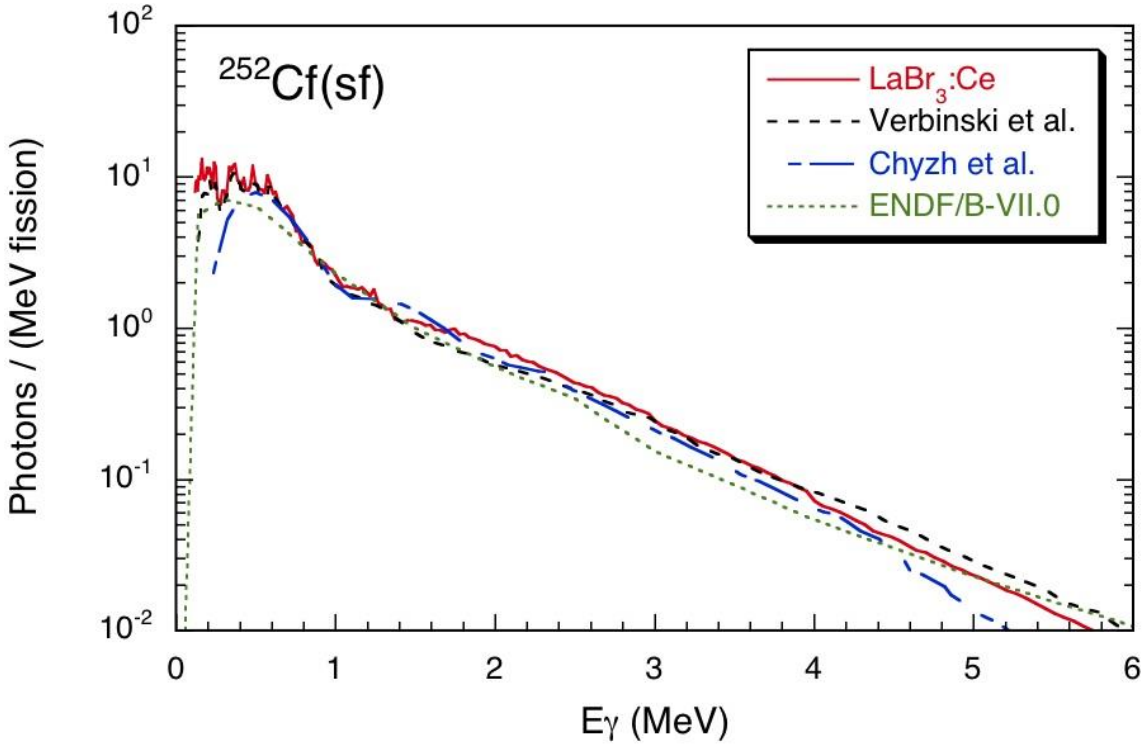

PRC 7 (1973)

PRC 85 (2012)

Below 1 MeV: good agreement with data from Verbinski (1973), but not with those from Chyzh (2012) and ENDF.

Results
^{252}Cf(sf) PFGS

R. Billnert et al., PRC 87 (2013)

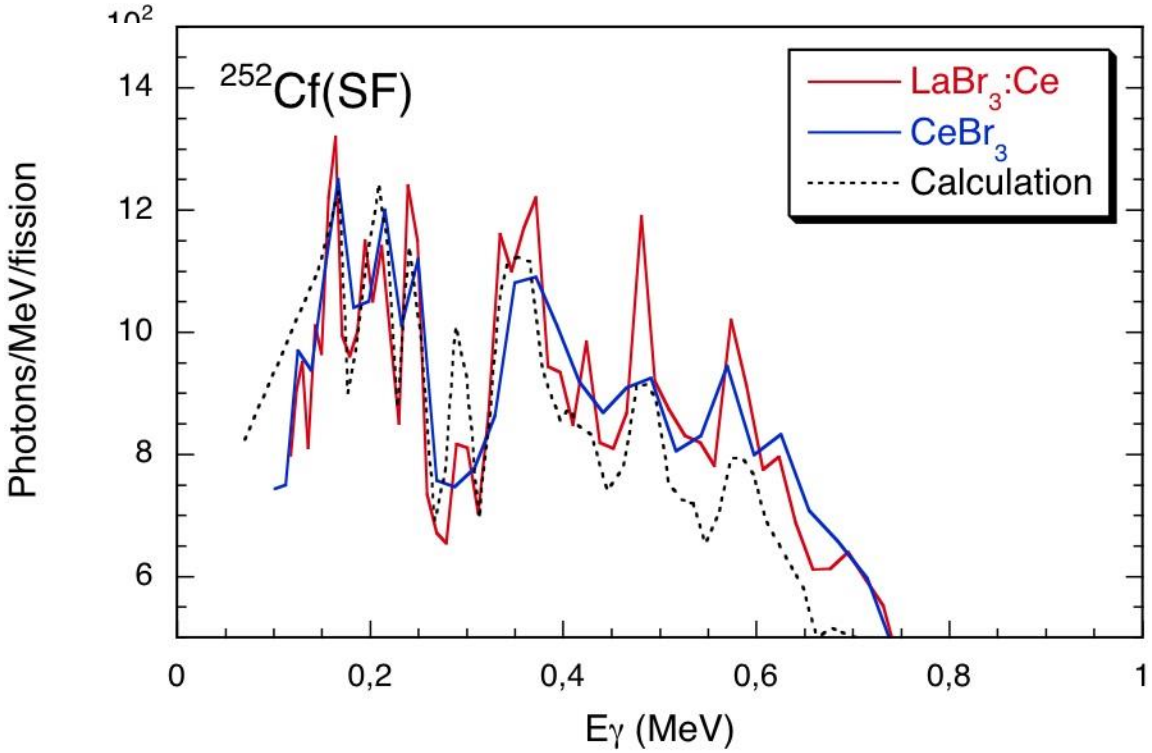

Good description provided by recent calculation *!

* full Hauser-Feshbach Monte Carlo simulation by D. Regnier (CEA Cadarache)

Results

^{252}Cf(sf) PFGS characteristics

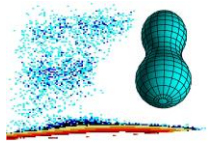

TABLE I. Summary of prompt γ-ray characteristics for the spontaneous fission of ^{252}Cf. Experimental results from this work for the γ-ray multiplicity ν_γ, the average energy ϵ_γ and the total energy $E_{\gamma,tot}$, obtained with three detectors employed in this work, are given and the covered energy range is indicated. Averaged values for the first two detectors are presented as well and compared to previously measured ones from Refs. [3–5] as well as corresponding numbers from the evaluated nuclear data files in ENDF/B-VII.1 [24] and from calculations from Ref. [11–13, 15, 25]. The results denoted by *) are calculated on the basis of the average values (see text for details).

Results	Detector	Diameter × length (in. × in.)	ν_γ (per fission)	ϵ_γ (MeV)	$E_{\gamma,tot}$ (MeV)	Energy range (MeV)	
This work *)	$LaBr_3$:Ce (Q489)	2 × 2	8.28 ± 0.08	0.80 ± 0.01	6.64 ± 0.10	0.1 - 7.2	
This work *)	$CeBr_3$ (315)	1 × 2	8.31 ± 0.10	0.80 ± 0.01	6.61 ± 0.12	0.1 - 6.5	
This work	$LaCl_3$:Ce (SEB 347)	1.5 × 1.5	8.25 ± 0.09	0.81 ± 0.02	6.60 ± 0.22	0.1 - 10.0	*)
This work	Averaged values		8.29 ± 0.06	0.80 ± 0.01	6.63 ± 0.08	> 0.1	
Chyzh *et al.* [3]	DANCE		8.14 ± 0.40	0.94 ± 0.05	7.65 ± 0.55	0.15 - 10.0	
Verbinski *et al.* [4]	NaI	2.3 × 6	7.80 ± 0.30	0.88 ± 0.04	6.84 ± 0.30	0.14 - 10.0	
Pleasonton *et al.* [5]	NaI	5 × 4	8.32 ± 0.40	0.85 ± 0.06	7.06 ± 0.35	> 0.085	
ENDF/B-VII.1 [24]	Evaluation		6.86	0.96	6.58	0.1 - 10.0	
Litaize *et al.* [13]	Calculation				6.77		
Regnier *et al.* [11]	Calculation		8.8	0.70	6.2	0.15 - 10.0	
Regnier [12]	Calculation		8.62	0.72	6.21	0.07 - 10.0	
Talou [25]	Calculation		7.96	0.86	6.85	0.14 - 10.0	
Becker *et al.* [15]	Calculation		9.97	0.85	8.47	0.14 - 10.0	

*) R. Billnert et al., PRC 87 (2013)

Results

^{252}Cf(sf) PFGS average multiplicity

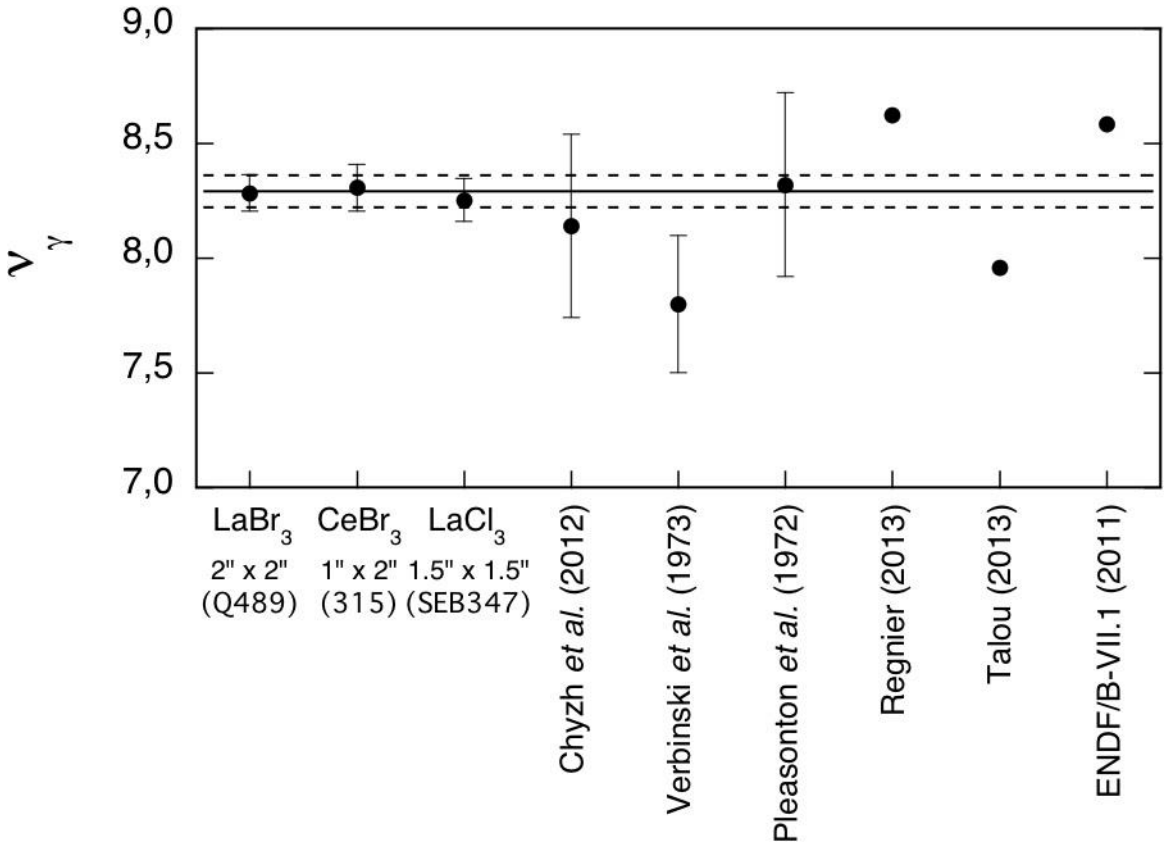

Results

^{252}Cf(sf) PFGS mean energy per photon

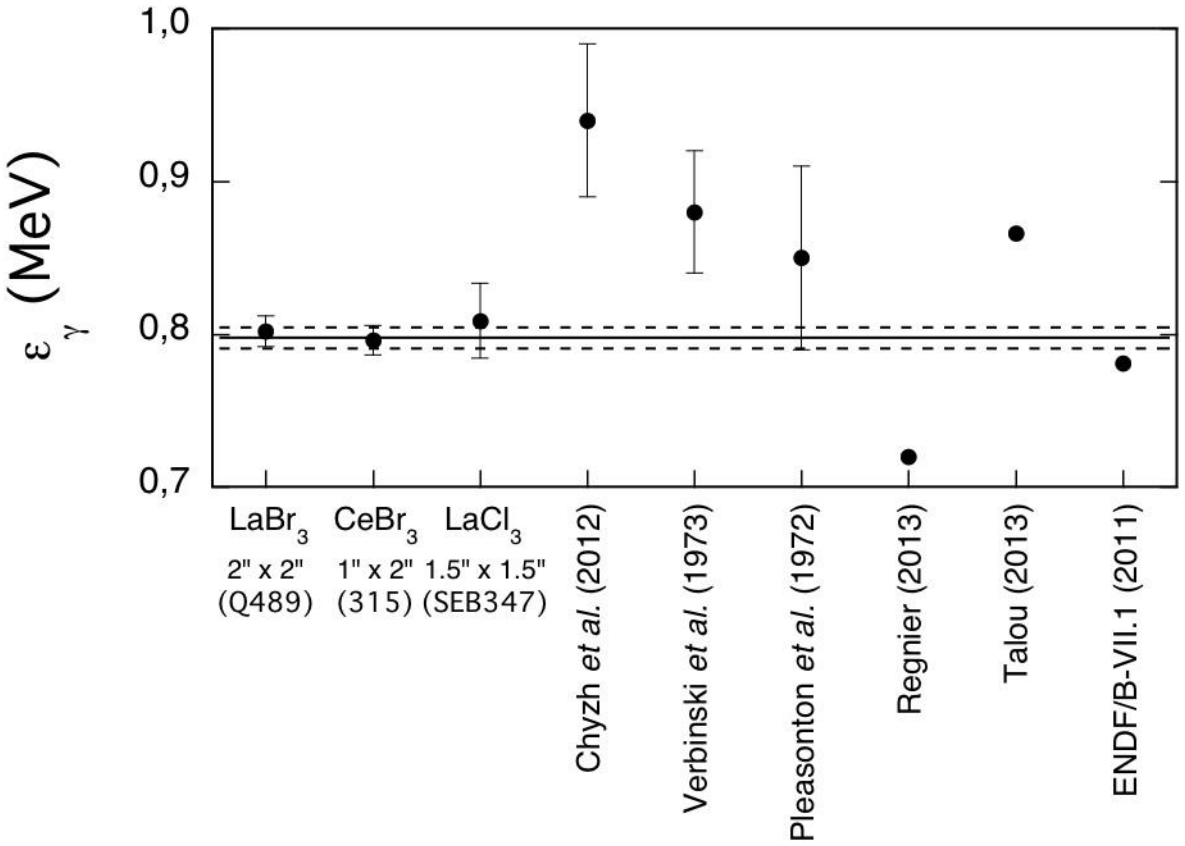

Results

^{252}Cf(sf) PFGS total energy per fission

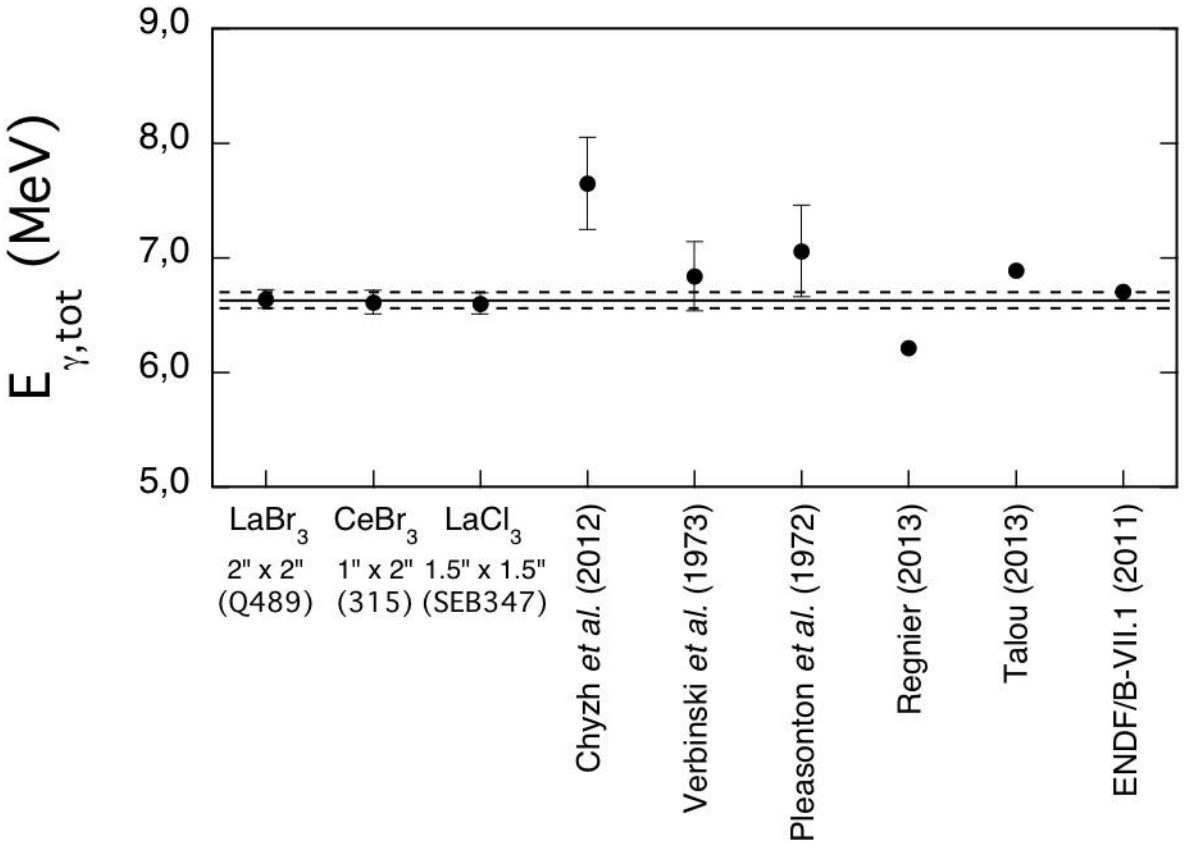

Results
PFGS

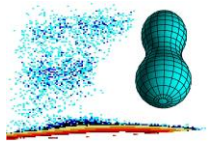

$^{235}U(n_{th}, f)$

Results
$^{235}U(n_{th}, f)$ PFGS

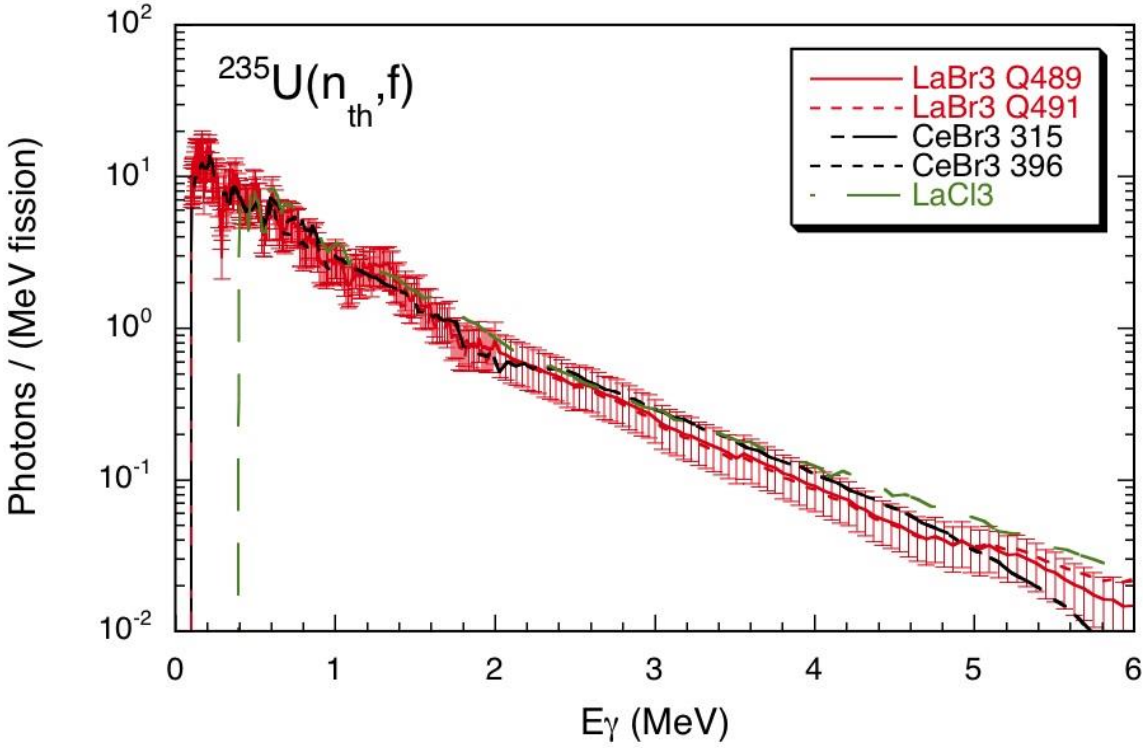

Excellent agreement between spectra taken with five different detectors at high energies …

Results
$^{235}U(n_{th}, f)$ PFGS

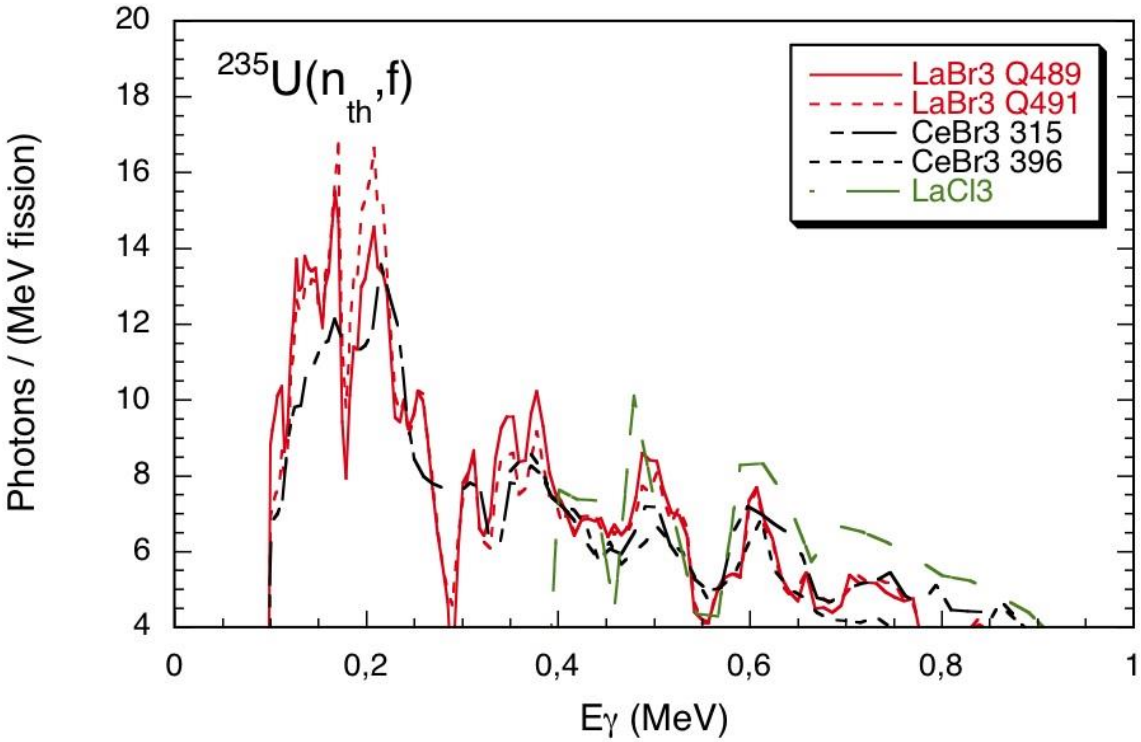

… as well as at low energies!

Results
$^{235}U(n_{th}, f)$ PFGS

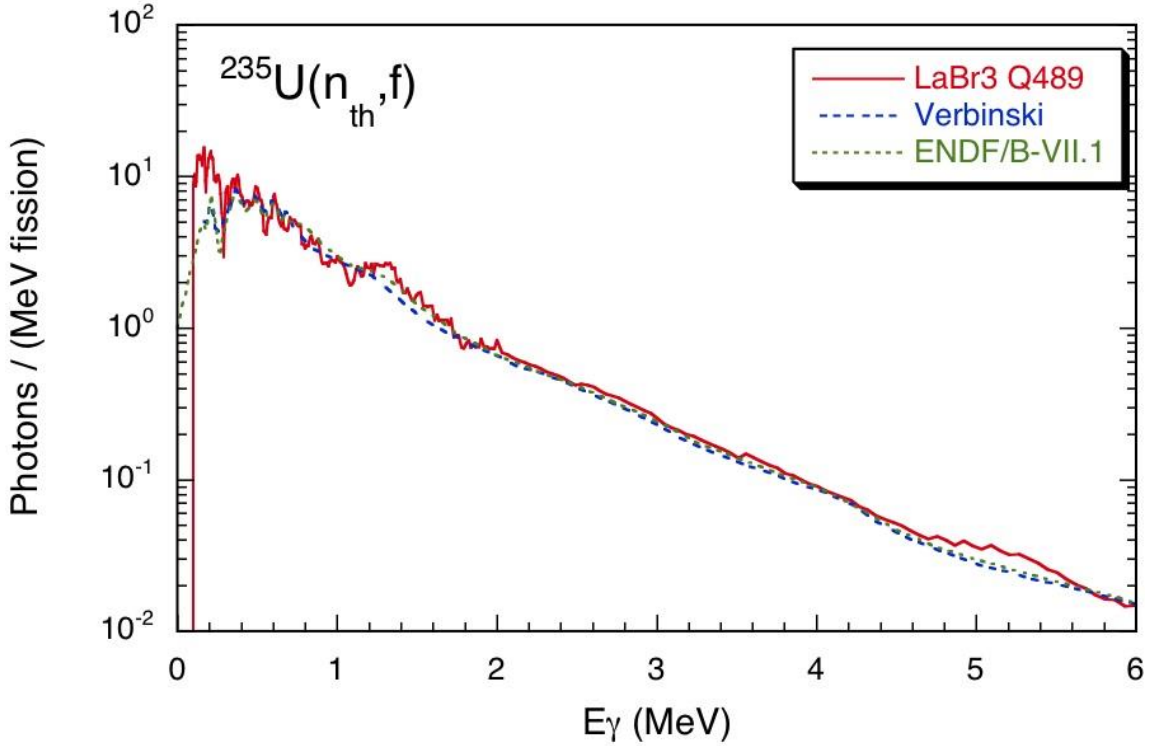

PRC 7 (1973)

Good agreement with data from both Verbinski (1973) and ENDF/B-VII.1, except for energies below 400 keV!

Results

$^{235}U(n_{th}, f)$ PFGS characteristics

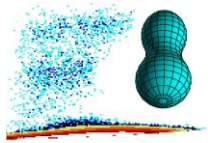

TABLE I. Summary of prompt γ-ray characteristics for the neutron-induced fission of ^{235}U. Experimental results from this work for the γ-ray multiplicity ν_γ, the average energy ϵ_γ and the total energy $E_{\gamma,tot}$, obtained with all five detectors employed in this work, are given and the covered energy range is indicated. Averaged values for the first three detectors are presented as well and compared to previously measured ones from Refs. [4–6] as well as corresponding numbers from the evaluated nuclear data files in ENDF/B-VII.1 [23] and from calculations from Ref. [14]. The results denoted by *) are calculated on the basis of the average values (see text for details).

Results	Detector	Diameter × length (in. × in.)	ν_γ (per fission)	ϵ_γ (MeV)	$E_{\gamma,tot}$ (MeV)	Energy range (MeV)	
This work	$LaBr_3$:Ce (Q489)	2 × 2	8.25 ± 0.17	0.84 ± 0.02	6.94 ± 0.14	0.1 - 6.0	
This work	$LaBr_3$:Ce (Q491)	2 × 2	8.09 ± 0.23	0.84 ± 0.03	6.79 ± 0.18	0.1 - 6.0	
This work	$CeBr_3$ (315)	1 × 2	8.16 ± 0.22	0.86 ± 0.03	7.03 ± 0.19	0.1 - 6.0	
This work	$CeBr_3$ (396)	1 × 2	7.94 ± 0.78	0.86 ± 0.09	6.81 ± 0.99	0.1 - 6.0	*)
This work	$LaCl_3$:Ce	3 × 3	8.21 ± 0.41	0.85 ± 0.05	6.99 ± 0.35	0.1 - 6.0	*)
This work	Averaged values		8.19 ± 0.11	0.85 ± 0.02	6.92 ± 0.09	0.1 - 6.0	
Verbinski *et al.* [4]	NaI	2.3 × 6	6.70 ± 0.30	0.97 ± 0.05	6.51 ± 0.30	0.14 - 10.0	
Pleasonton *et al.* [5]	NaI	5 × 4	6.51 ± 0.30	0.99 ± 0.07	6.43 ± 0.30	0.09 - 10.0	
Peelle *et al.* [6]	NaI	1.75 × 1	7.45 ± 0.35	0.96	7.18 ± 0.26	0.14 - 10.0	
ENDF/B-VII.1 [23]	Evaluation		6.86	0.96	6.58	0.1 - 10.0	
Becker *et al.* [14]	Calculation		8.05	0.88	7.06	0.14 - 10.0	

A. Oberstedt et al., PRC 87 (2013)

Results

$^{235}U(n_{th}, f)$ PFGS average multiplicity

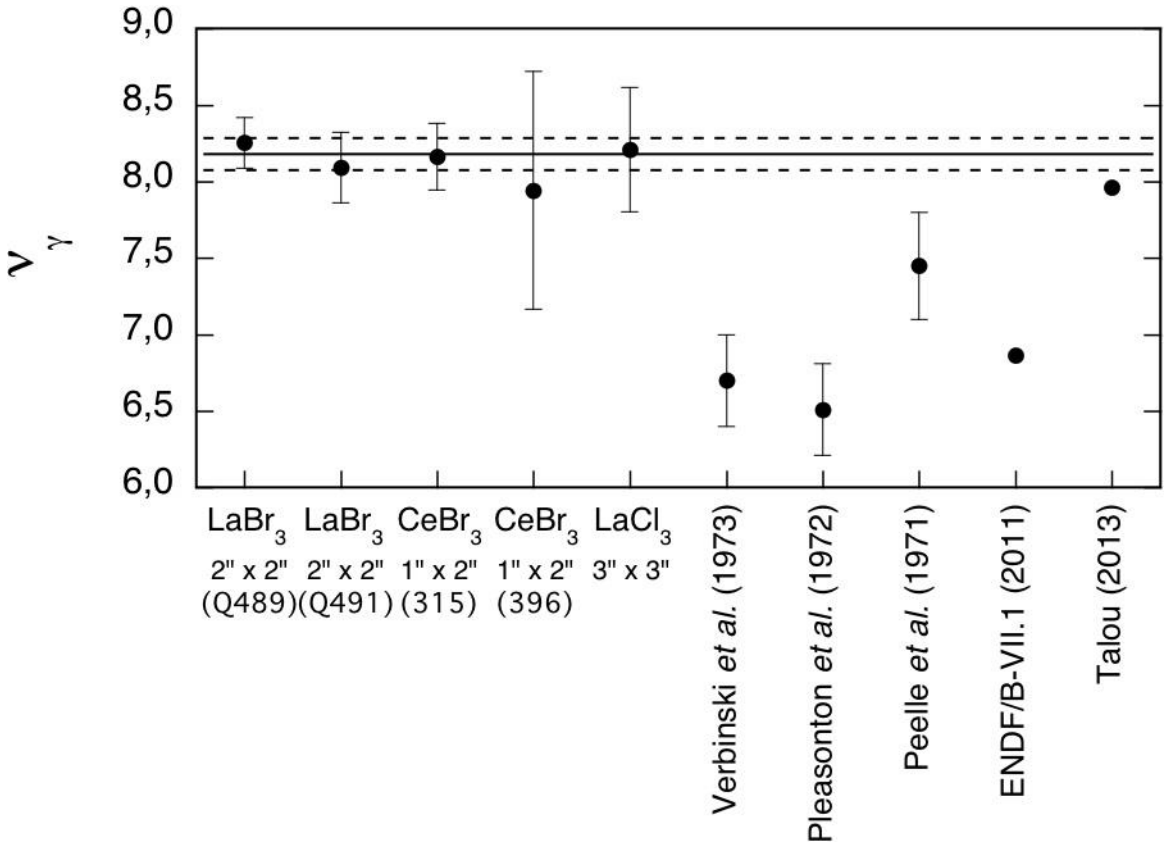

Results

$^{235}U(n_{th}, f)$ PFGS mean energy per photon

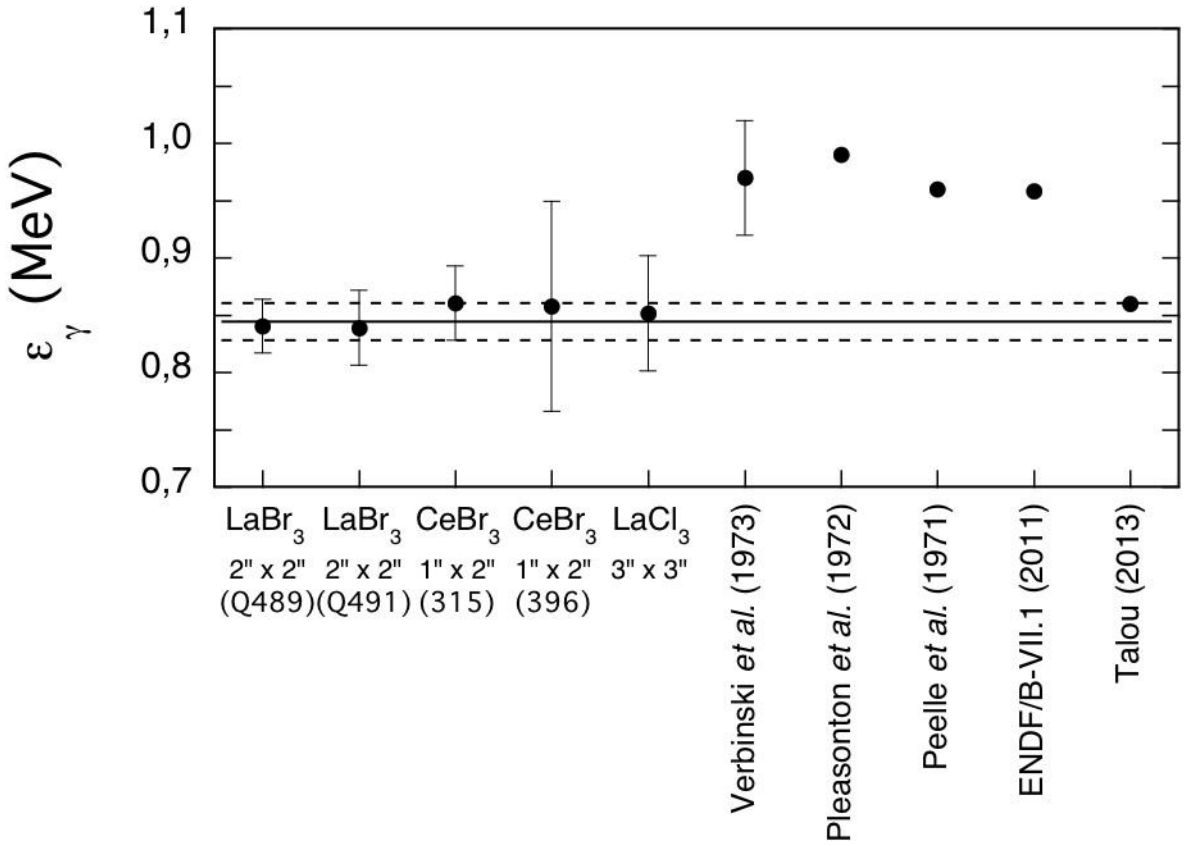

Results

$^{235}U(n_{th}, f)$ PFGS total energy per fission

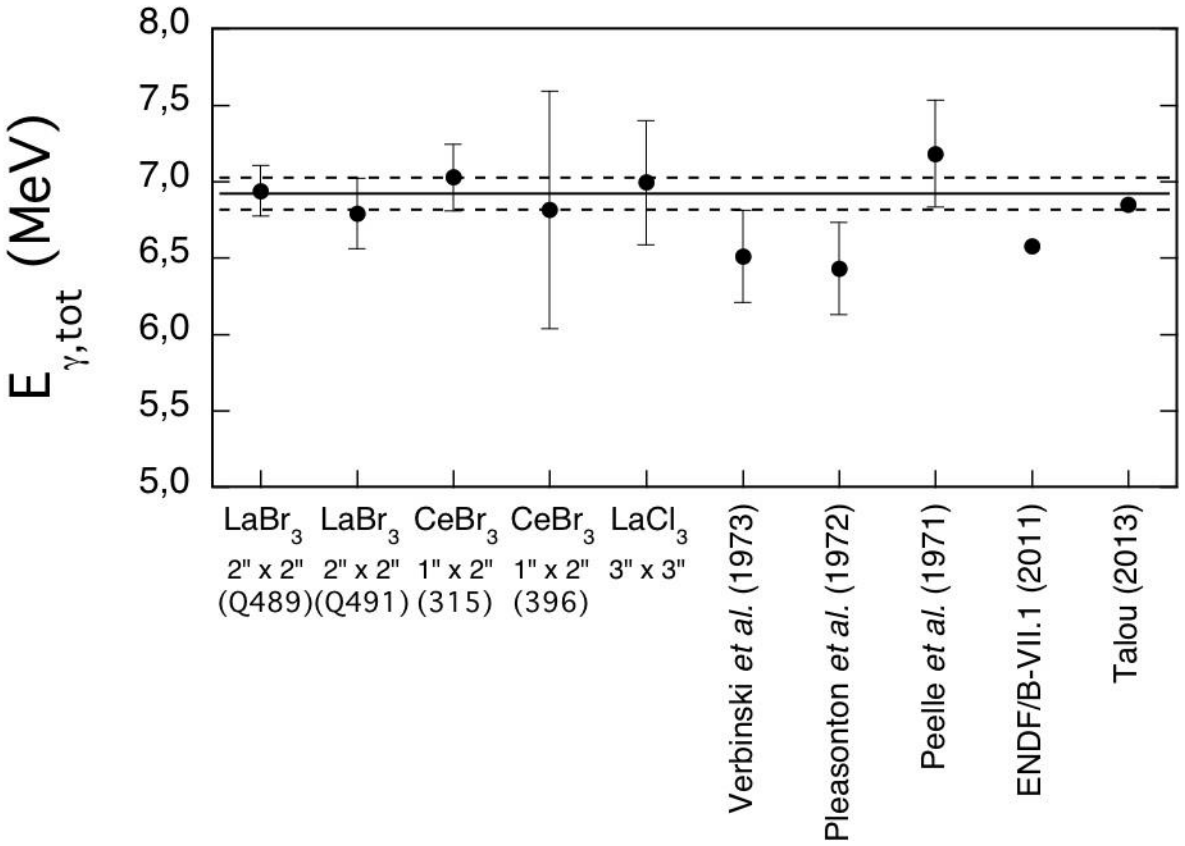

Results

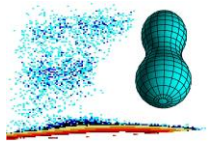

$^{241}Pu(n_{th}, f)$

Results
$^{241}Pu(n_{th}, f)$ PFGS

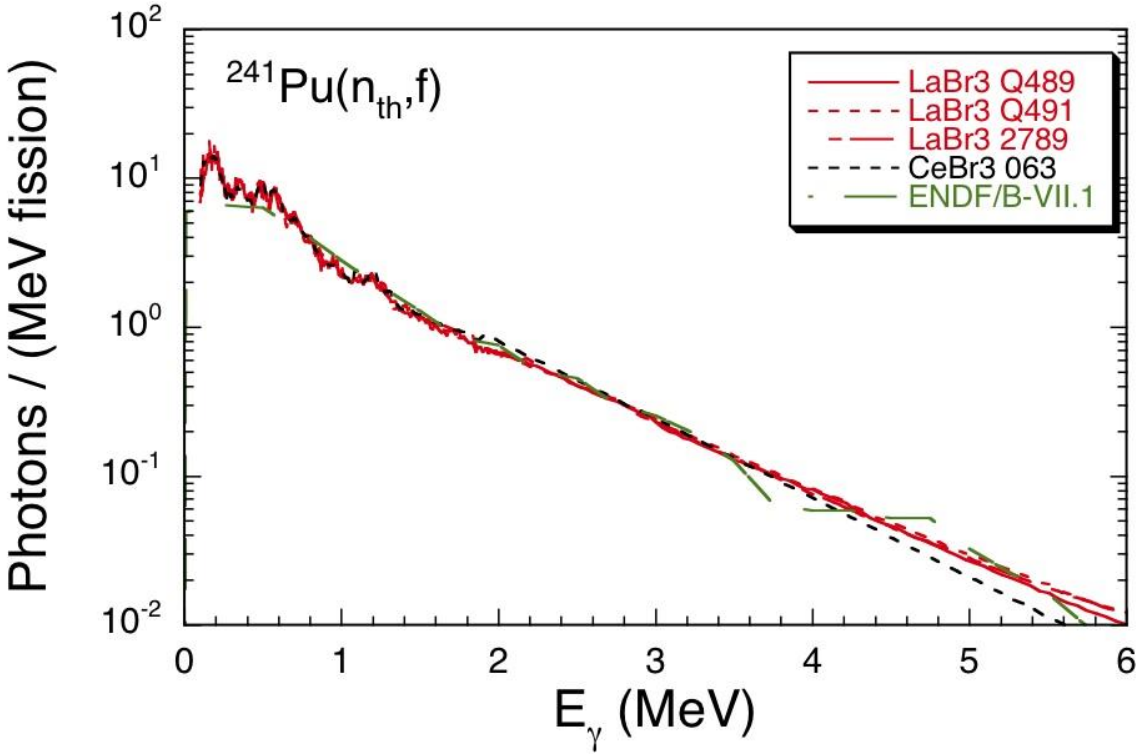

Excellent agreement between spectra taken with four different detectors over the entire energy range, compared to ENDF/B-VII.1.

Results

$^{241}Pu(n_{th}, f)$ PFGS characteristics

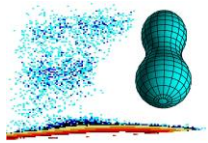

TABLE II. Summary of prompt γ-ray characteristics for the neutron-induced fission of ^{241}Pu. Experimental results from this work for the average γ-ray multiplicity $\overline{\nu}_\gamma$, the average energy ϵ_γ and the total energy $E_{\gamma,tot}$, obtained with all five detectors employed in this work, are given and the covered energy range is indicated. Averaged values for the four detectors are presented as well and compared to the evaluated nuclear data files in ENDF/B-VII.1 [11] and recent data from Chyzh et al.[21]. The uncertainties on their mean values, denoted by *), were estimated from discussed uncertainties in there.

Results	Detector	Diameter × length (cm × cm)	$\overline{\nu}_\gamma$ (per fission)	ϵ_γ (MeV)	$E_{\gamma,tot}$ (MeV)	Energy range (MeV)	
This work	$LaBr_3$:Ce (Q489)	5.08 × 5.08	8.20 ± 0.17	0.78 ± 0.02	6.41 ± 0.12	0.1 - 6.0	
This work	$LaBr_3$:Ce (Q491)	5.08 × 5.08	8.19 ± 0.17	0.78 ± 0.02	6.41 ± 0.12	0.1 - 6.0	
This work	$CeBr_3$ (063)	5.08 × 5.08	8.23 ± 0.20	0.79 ± 0.03	6.48 ± 0.15	0.1 - 6.0	
This work	$LaBr_3$:Ce (2789)	7.62 × 7.62	8.23 ± 0.17	0.78 ± 0.02	6.38 ± 0.11	0.1 - 6.0	
This work	Averaged values		8.21 ± 0.09	0.78 ± 0.01	6.41 ± 0.06	0.1 - 6.0	
ENDF/B-VII.1 [11]	Evaluation		8.18	0.76	6.19	0.1 - 10.0	
Chyzh *et al.* [21]	DANCE (BaF_2)		7.5 ± 0.3	0.92 ± 0.06	6.90 ± 0.53	0.15 - 9.5	*)

manuscript, to be published

Results

$^{241}Pu(n_{th}, f)$ PFGS average multiplicity

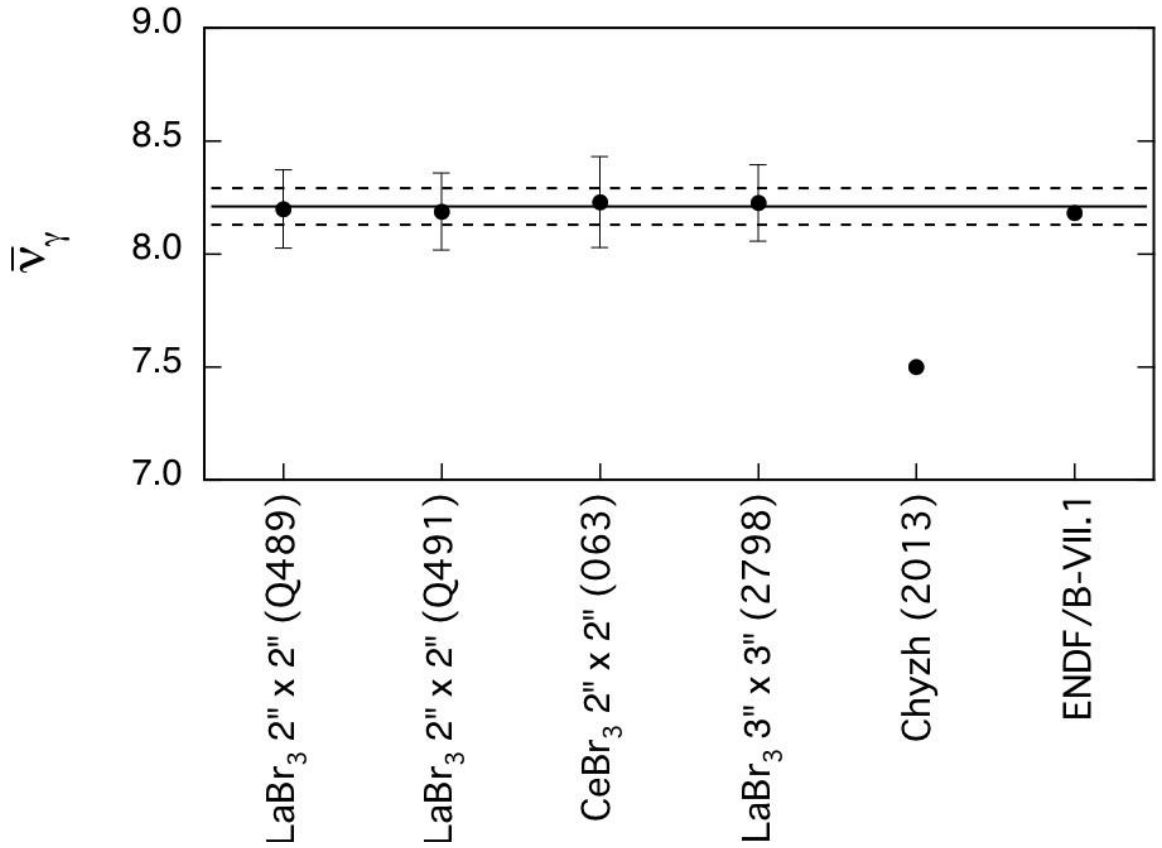

Results

$^{241}Pu(n_{th}, f)$ PFGS mean energy per photon

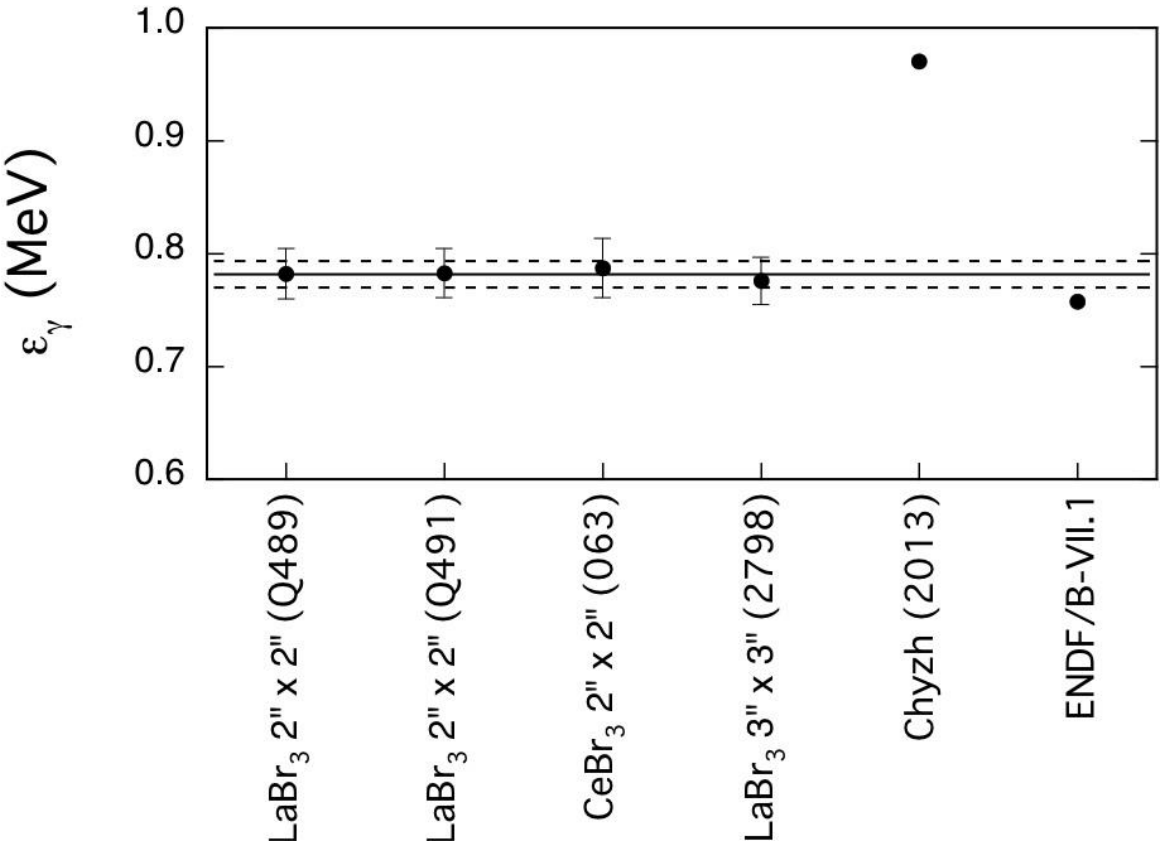

Results

$^{241}Pu(n_{th}, f)$ PFGS total energy per fission

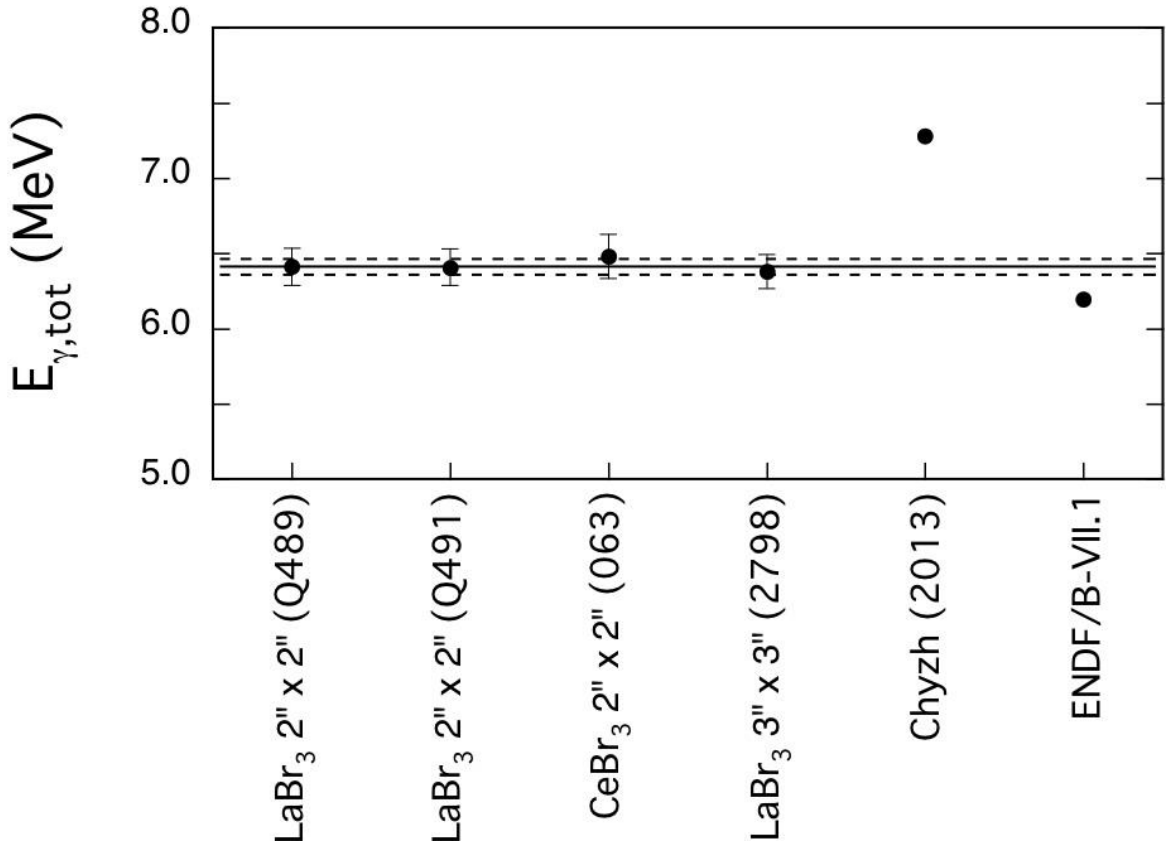

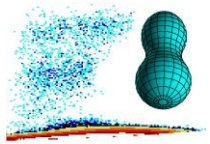

Summary

Outlook

Summary

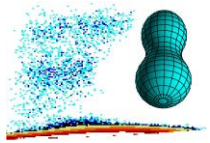

- Prompt fission γ-ray spectra (PFGS) measured for ^{252}Cf(sf), ^{235}U(n_{th}, f) and ^{241}Pu(n_{th}, f)
- Lanthanide halide crystal scintillation detectors well suited for these measurements
  - excellent timing resolution (<< 1ns)
  - good energy resolution (3-4% at 662 keV)
- n/γ discrimination by time-of-flight
- Improved results on PFGS characteristics (multiplicity, mean and total energies)
  - much higher precision than required for Gen-IV reactor core modelling (7.5% on energy)
- Neutron measurements possible with threshold < 300 keV (standard detectors: 0.5 – 1 MeV)

Outlook

Comparison: $^{235}U(n_{th},f)$, $^{241}Pu(n_{th},f)$ and $^{252}Cf(sf)$

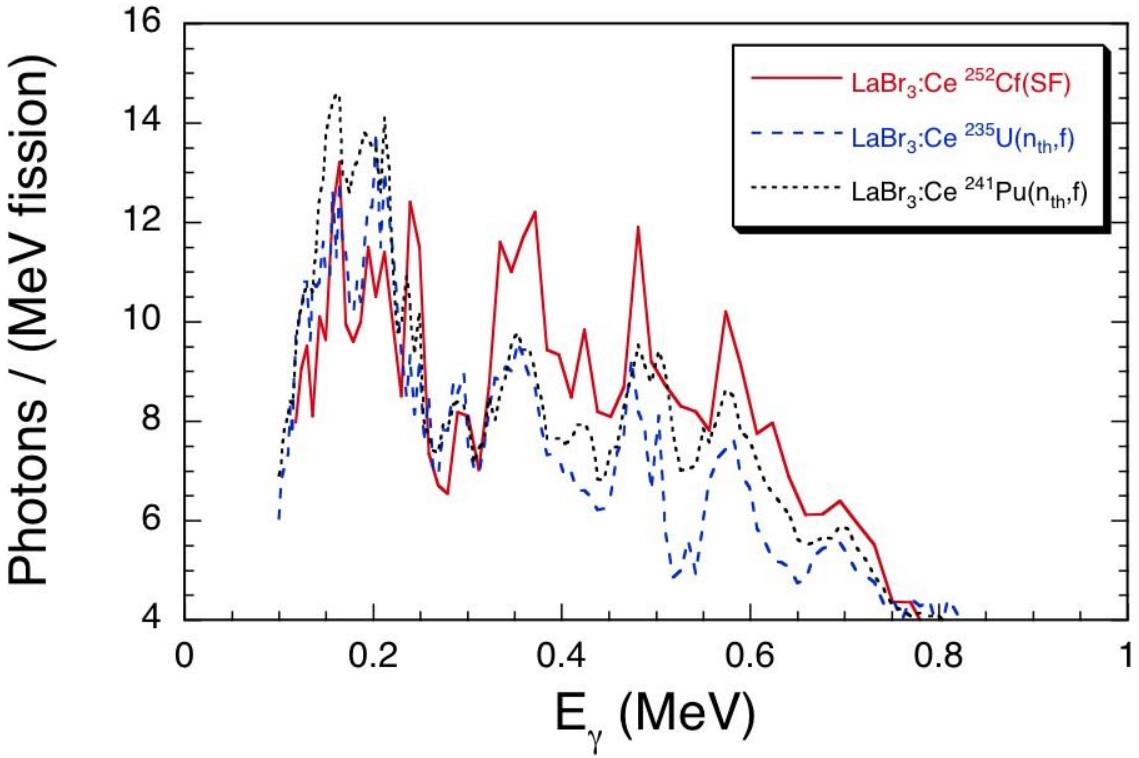

Similar low energy structure in all three fissioning systems

→ decay of rotational states in the same heavy fragments?

Outlook

Comparison: $^{235}U(n_{th},f)$, $^{241}Pu(n_{th},f)$ and $^{252}Cf(sf)$

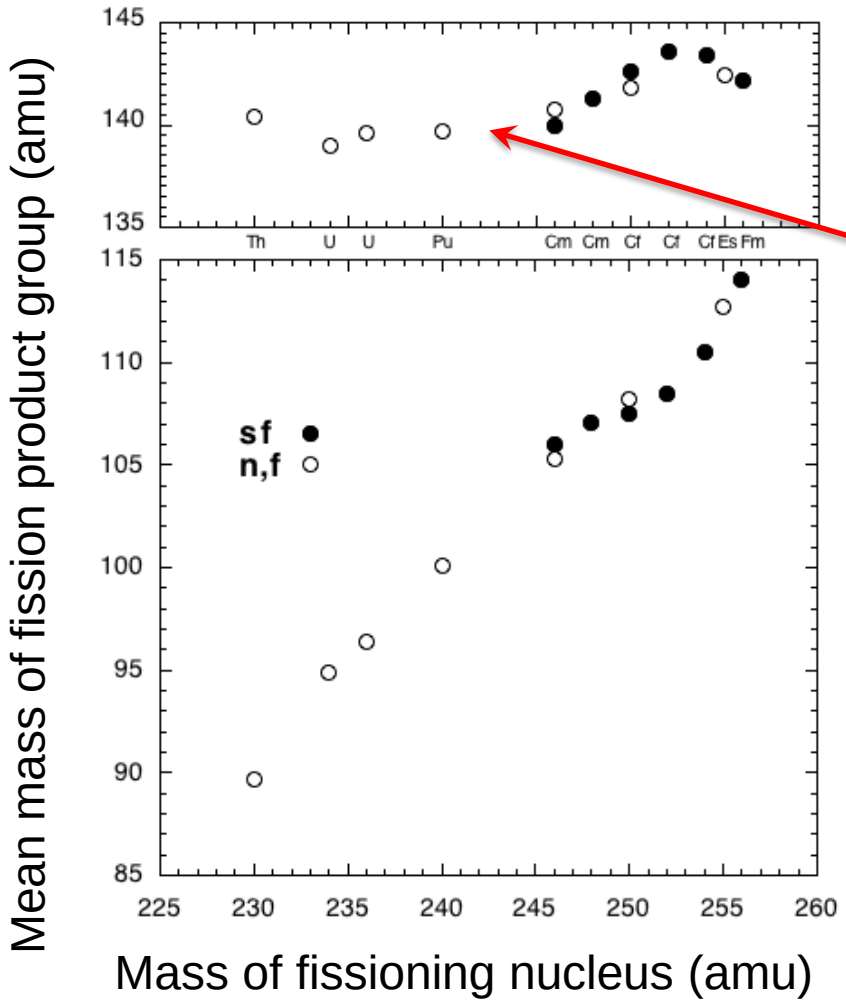

Heavy fragments

Hint: about the same mean mass!

Light fragments

Outlook

Comparison: $^{235}U(n_{th},f)$, $^{241}Pu(n_{th},f)$ and $^{252}Cf(sf)$

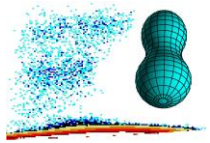

Approach:

- correlation measurements of prompt fission γ-rays with fragment mass (and energy)
- comparison of our experimental data with results from full Hauser-Feshbach Monte Carlo calculations for both fissioning systems by
  - CEA Cadarache group (O. Serot, O. Litaize and D. Regnier)
  - Los Alamos / New York collaboration (P.Talou, B. Becker et al.)

Outlook
New experiments

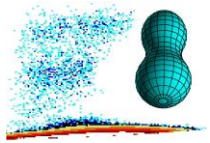

- Correlated PFGS (and PFNS) from ^{252}Cf(sf) at IRMM
  - going on
  - array with 10 γ-ray detectors
  - digital DAQ
  - test for Budapest experiment

- Analysis of PFNS data from the ^{235}U(n_{th}, f) and ^{241}Pu(n_{th}, f) experiments in Budapest in 2012 and 2013

The collaborators

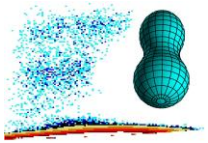

R. Billnert, A. Oberstedt, S. Oberstedt

with invaluable support of

T. Belgya, R. Borcea, T. Bryś, C. Chaves, Th. Gamboni, W. Geerts,

A. Göök, C. Guerrero, F.-J. Hambsch, Z. Kis, T. Martinez,

L. Szentmiklosi, K. Takács, M. Vidali

**This work was supported by
the ERINDA programme (agreement number 269499) and
the EFNUDAT programme (agreement number 31027)
of the European Commission**

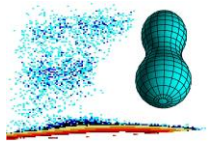

Thank you!